Analysis of a pattern-forming lattice-gas automaton: Mean-field theory and beyond

Harmen J. Bussemaker*
Institute for Theoretical Physics, University of Utrecht, P.O. Box 80.006, Utrecht, The Netherlands
(Received 4 May 1995)

An analysis is presented of a two-dimensional lattice model of random walkers that interact through a nearest neighbor attraction. The model exhibits a dynamical phase transition to a spatially unstable state, leading to pattern formation and domain coarsening. A mean-field theory is formulated. It is applied to predict the critical temperature and to explain observed anisotropic behavior. The occurrence of a striped phase in the presence of an external driving field is clarified, and a linear response theorem relating the induced particle flux to the variance of equilibrium fluctuations is derived. To account for deviations from mean-field theory, an Enskog-Boltzmann equation is derived that accounts for the effect of static pair correlations existing in equilibrium due to the lack of detailed balance. For temperatures above the critical temperature we obtain corrections to mean-field theory for the diffusion coefficient. Below the critical temperature the theory is used to explain the initial stages of phase separation.

PACS number(s): 05.20.Dd, 05.60.+w, 05.70.Ln

I. INTRODUCTION

Pattern formation occurs in lattice-gas automata (LGA) for immiscible fluids [1], liquid-gas transitions [2], reaction-diffusion systems [3,4], and traffic jams [5,6]. A great advantage of LGA over continuum descriptions, like partial differential equations or lattice-BGK (i.e., single relaxation time) models [7–9], is that due to their Boolean nature LGA possess intrinsic fluctuations. Since in most cases pattern formation results from the amplification of microscopic fluctuations in a spatially homogeneous initial state, due to unstable macroscopic diffusive or hydrodynamic modes, LGA are ideally suited to a mesoscopic study of pattern formation phenomena where both aspects are important. Each cell on the lattice plays the role of a volume element that is large enough to contain a considerable number of microscopic particles, but on the other hand is small compared to all macroscopic length scales in the system.

A feature that is shared by almost all pattern-forming LGA is *lack of detailed balance.* When a LGA satisfies detailed balance its equilibrium state is completely described by the Gibbs distribution known from standard statistical mechanics. The Gibbs distribution is universal, in the sense that it only depends on the microscopic state through global invariants like the total number of particles. When a model lacks detailed balance the equilibrium distribution is non-Gibbsian and depends on the details of the microscopic collision rules. There exist (often strong) spatial correlations between microscopic variables, which affect the macroscopic behavior of the model. Therefore it is important to understand these correlations theoretically.

A first step towards a theory for non-detailed-balance LGA was made by Bussemaker, Ernst, and Dufty [10]. They derived approximate equations for the coupled time evolution of the single particle distribution function and the pair correlation function, by neglecting all third and higher order correlations. By considering a stationary solution to these kinetic equations an estimate for the pair correlation function in equilibrium was obtained, in good agreement with simulation results.

Even in LGA that satisfy detailed balance there are effects of *dynamic correlations* that are generated when a nonequilibrium state relaxes towards equilibrium. The contribution of ring collisions to transport coefficients was first calculated by Ernst and co-workers [11–16]. No theory beyond the mean-field approximation exists for transport coefficients in LGA that lack detailed balance.

The present article provides a theory for transport coefficients that takes equilibrium pair correlations into account in the simplest possible manner. All dynamic correlations and higher order static correlations are neglected. We expect that for models that strongly violate detailed balance the dominant correction to mean-field theory comes from the static pair correlations.

We analyze a two-dimensional diffusive model introduced by Alexander, Edrei, Garrido, and Lebowitz [17] as a limiting case of the immiscible fluid LGA of Rothman and Keller [1]. Random walkers interact through nearest neighbor attraction. The strength of the interaction is tuned by a temperaturelike parameter. For each value of the initial uniform density, there exists a critical temperature where a dynamical phase transition occurs, from a spatially homogeneous equilibrium state to a phase separated state where high and low density phases coexist. At temperatures below the critical temperature the spatially uniform state is unstable against long wavelength excita-

*Present address: Institute for Physical Science and Technology, University of Maryland, College Park, MD 20742; email: harmen@ipst.umd.edu.

tions. The system tries to reach the two-phase equilibrium state by a process of coarsening, during which the typical size of domains grows in time so that local equilibrium is reached on a larger and larger spatial scale.

The organization of this article is as follows. In Sec. II we define the model. In Sec. III the model is analyzed in the mean-field approximation. The resulting nonlinear Boltzmann equation is a closed time evolution equation for the single particle distribution function. By analyzing the behavior of small deviations from equilibrium, we obtain an expression for the diffusion coefficient as a function of the macroscopic parameters (density and temperature), and we calculate the critical temperature in mean-field approximation. The eigenvalue spectrum of the linearized Boltzmann collision operator contains information about the typical length and time scales at the onset of phase separation, and about the isotropy of the patterns. In Sec. IV the effect of an external driving field on the behavior of the model is analyzed in mean-field approximation. A linear response relation is derived for the induced particle flux, and the occurrence of striped patterns is explained using the eigenvalue spectrum.

Section V starts with the derivation of a ring kinetic theory for the static pair correlations in equilibrium, along the lines of Ref. [10]. By expanding the master equation around mean-field theory an Enskog-Boltzmann equation is derived that is used to estimate the corrections to the diffusion coefficient due to the equilibrium pair correlations. Finally in Sec. VI the Enskog theory is applied to predict the time evolution of the static structure factor during the initial stages of coarsening. For large times the predictions of dynamic scaling are tested. We end with a discussion in Sec. VII.

II. THE MODEL

We consider a lattice-gas automaton (LGA) defined on a two-dimensional lattice with periodic boundary conditions. Let b denote the coordination number: on the square lattice $b = 4$ and on the triangular lattice $b = 6$. There are $V = L \times L$ nodes in the lattice, labeled $\mathbf{r}$. At each node there is room for up to b particles in the velocity channels $\mathbf{c}_i = (\cos 2\pi(i-1)/b, \sin 2\pi(i-1)/b)$ with $1 \leq i \leq b$ corresponding to nearest neighbor vectors. A channel $(\mathbf{r}, \mathbf{c}_i)$ can either be empty or occupied by at most one particle with velocity $\mathbf{c}_i$. The state of the entire lattice at time t is denoted by a set of occupation numbers $s_i(\mathbf{r}, t) = 0, 1$ denoting the absence or presence, respectively, of a particle in channel $(\mathbf{r}, \mathbf{c}_i)$.

A time evolution step in the model consists of a *collision step* followed by a *propagation step*. The collision step transforms a precollision state $s_i(\mathbf{r}, t)$ into a postcollision state $\sigma_i(\mathbf{r}, t)$ according to stochastic collision rules. During the propagation step all particles are moved to nearest neighbors in the direction of their velocity. In terms of occupation numbers this is represented by

$$s_i(\mathbf{r} + \mathbf{c}_i, t+1) = \sigma_i(\mathbf{r}, t). \tag{1}$$

Let the number of particles at node $\mathbf{r}$ be denoted by

$$\rho(\mathbf{r}, t) = \sum_{i=1}^{b} s_i(\mathbf{r}, t). \tag{2}$$

During collision the number of particles at each node $\mathbf{r}$ must remain constant,

$$\sum_{i=1}^{b} \sigma_i(\mathbf{r}, t) = \sum_{i=1}^{b} s_i(\mathbf{r}, t), \tag{3}$$

i.e., no creation or annihilation of particles is allowed. There are no other constraints. Before the collision step can be performed the gradient field in the local density,

$$\mathbf{G}(\mathbf{r}, t) = \sum_{p=1}^{b} \mathbf{c}_p \, \rho(\mathbf{r} + \mathbf{c}_p, t), \tag{4}$$

must be calculated from the local densities $\rho(\mathbf{r} + \mathbf{c}_p, t)$ at the b neighbors of each node. The collision rules are defined in such a way that particles preferably move in the direction of increasing density, i.e., parallel to $\mathbf{G}$, which mimics attraction between particles and gives rise to antidiffusion. The degree of preference is tuned by a temperaturelike parameter $T \equiv 1/\beta$. Let the particle flux $\mathbf{J}(\sigma)$ corresponding to a postcollision state σ at a single node be given by

$$\mathbf{J}(\sigma) = \sum_{i=1}^{b} \mathbf{c}_i \, \sigma_i. \tag{5}$$

The probability that σ is the outcome of a collision at node $\mathbf{r}$, when s is the precollision state at $\mathbf{r}$ and $\mathbf{G}(\mathbf{r})$ the local density gradient, is given by

$$A_{s\sigma}(\mathbf{G}(\mathbf{r})) = \frac{1}{Z(s)} e^{\beta \mathbf{G}(\mathbf{r}) \cdot \mathbf{J}(\sigma)} \delta(\rho(s), \rho(\sigma)), \tag{6}$$

where δ denotes the Kronecker symbol. The normalization constant is given by

$$Z(s) = \sum_{\sigma} e^{\beta \mathbf{G}(\mathbf{r}) \cdot \mathbf{J}(\sigma)} \delta(\rho(s), \rho(\sigma)). \tag{7}$$

In the limit of *high* temperature ($\beta = 0$) the gradient $\mathbf{G}$ does not have any effect on the outcome of the collision: the outcome σ is chosen with equal probability among all states that have the right number of particles $\rho(\sigma) = \rho(s)$. In this limit a random walker model is obtained with a positive diffusion coefficient. In the limit of *low* temperature ($\beta = \infty$) the outcome σ is chosen among the smaller subset of states that make the inner product $\mathbf{J}(\sigma) \cdot \mathbf{G}(\mathbf{r})$ maximal. As it turns out, in this case the diffusion coefficient is negative, leading to spatial instability and pattern formation. There is a critical temperature $T_c = 1/\beta_c$ where the diffusion coefficient changes sign from positive to negative. The former case is stable; the latter is unstable against large scale density fluctuations and leads to phase separation for $\beta > \beta_c$. One of the main goals of this article is a calculation of β_c.

III. BOLTZMANN THEORY

A. The nonlinear Boltzmann equation

Let $n_i(\mathbf{r},t)$ denote the microscopic state of the system in a way analogous to $s_i(\mathbf{r},t)$. The state $\{n(\mathbf{r},t)\}$ of all nodes of the lattice simultaneously can be thought of as a point in a discrete *phase space* consisting of all 2^{bV} possible different microstates. Since we are interested in the time evolution of an ensemble of microstates it is convenient to introduce a probability distribution on this phase space: $p(\{n(\mathbf{r},t)\},t)$. We define $\langle\cdots\rangle$ as the ensemble average,

$$\langle\cdots\rangle \equiv \sum_{\{n(\mathbf{r},t)\}} (\cdots)\; p(\{n(\mathbf{r},t)\},t). \tag{8}$$

A formal expression for the phase space distribution is then given by

$$\begin{aligned} p(\{s(\mathbf{r})\},t) &= \left\langle \prod_{\mathbf{r},i} \delta(s_i(\mathbf{r}), n_i(\mathbf{r},t)) \right\rangle \\ &= \left\langle \prod_{\mathbf{r},i} n_i(\mathbf{r},t)^{s_i(\mathbf{r})}[1-n_i(\mathbf{r},t)]^{1-s_i(\mathbf{r})} \right\rangle . \end{aligned} \tag{9}$$

Although it is straightforward to write down the master equation that describes the time evolution of $p(\{s(\mathbf{r})\},t)$, this equation is of little use if one wants to calculate transport quantities like the diffusion coefficient. It keeps track of all information about the state of the system, which makes it completely intractable.

The average equation of motion for the *single particle distribution function*,

$$f_i(\mathbf{r},t) = \langle s_i(\mathbf{r},t)\rangle , \tag{10}$$

can be constructed by averaging Eq. (1) over an arbitrary initial ensemble, with the result

$$f_i(\mathbf{r}+\mathbf{c}_i,t+1) - f_i(\mathbf{r},t) = \langle \sigma_i(\mathbf{r},t) - s_i(\mathbf{r},t)\rangle , \tag{11}$$

where the collision term on the right hand side is defined as

$$\begin{aligned} \langle \sigma_i(\mathbf{r},t) - s_i(\mathbf{r},t)\rangle \;=\; & \sum_{\{\sigma(\mathbf{r})\}} \sum_{\{s(\mathbf{r})\}} [\sigma_i(\mathbf{r}) - s_i(\mathbf{r})] \\ & \times \left(\prod_{\mathbf{r}} A_{s(\mathbf{r}),\sigma(\mathbf{r})}(\mathbf{G}(\mathbf{r})) \right) \\ & \times p(\{s(\mathbf{r})\},t). \end{aligned} \tag{12}$$

The simplest approximation to the master equation, which, however, captures the essential physics and often provides surprisingly good predictions is the *Boltzmann approximation* or *mean-field approximation* (*Stosszahlansatz*), in which fluctuations are neglected and distribution functions are completely factorized. It amounts to discarding all information contained in $p(\{s(\mathbf{r})\},t)$, except for the single particle distribution function, and approximating $p(\{s(\mathbf{r})\},t)$ by the *completely factorized distribution*

$$p(\{s(\mathbf{r})\},t) = \prod_{\mathbf{r},i} [f_i(\mathbf{r},t)]^{s_i}[1-f_i(\mathbf{r},t)]^{1-s_i}, \tag{13}$$

so that all pair, triplet, and higher order correlations are neglected. The factors $f_i(\mathbf{r},t)$ and $1-f_i(\mathbf{r},t)$ are a consequence of the Fermi exclusion rule and account for the probabilities of finding, respectively, a particle and a hole in channel $(\mathbf{r},\mathbf{c}_i)$.

We define $\langle\,\rangle_{\mathrm{MF}}$ as a mean-field average for observables that depend on both the precollision state $\{s(\mathbf{r})\}$ and the postcollision state $\{\sigma(\mathbf{r})\}$ at time t,

$$\begin{aligned} \langle\cdots\rangle_{\mathrm{MF}} \equiv & \sum_{\{\sigma(\mathbf{r})\}} \sum_{\{s(\mathbf{r})\}} (\cdots) \\ & \times \prod_{\mathbf{r}} \left[A_{s(\mathbf{r}),\sigma(\mathbf{r})}(\mathbf{G}(\mathbf{r})) F(s(\mathbf{r}),\mathbf{r},t) \right] , \end{aligned} \tag{14}$$

with the factorized single node distribution $F(s,\mathbf{r},t)$ defined as

$$F(s,\mathbf{r},t) = \prod_i [f_i(\mathbf{r},t)]^{s_i}[1-f_i(\mathbf{r},t)]^{1-s_i}. \tag{15}$$

In Eq. (14) the distribution over postcollision states is obtained by applying the collision matrix $A_{s\sigma}(\mathbf{G})$ to the completely factorized precollision distribution Eq. (13) for all nodes in the lattice. Note that when $\beta \neq 0$ the postcollision distribution contains correlations between occupation numbers at the same node and at nearest neighbor nodes, due to the asymmetry resulting from the biasing factor in Eq. (6). By using the normalization $\sum_\sigma A_{s\sigma}(\mathbf{G}) = 1$, it can be verified that $\langle s_i(\mathbf{r},t)\rangle_{\mathrm{MF}} = f_i(\mathbf{r},t)$.

We obtain a closed evolution equation for $f_i(\mathbf{r},t)$ by using the Boltzmann approximation, i.e., by replacing the average $\langle\,\rangle$ in Eq. (11) by $\langle\,\rangle_{\mathrm{MF}}$. We obtain the well-known *nonlinear Boltzmann equation*,

$$f_i(\mathbf{r}+\mathbf{c}_i,t+1) - f_i(\mathbf{r},t) \simeq \Omega_i^{10}(\mathbf{r},t), \tag{16}$$

with the nonlinear collision operator Ω_i^{10} defined by

$$\Omega_i^{10}(\mathbf{r},t) \equiv \langle \sigma_i(\mathbf{r},t) - s_i(\mathbf{r},t)\rangle_{\mathrm{MF}} . \tag{17}$$

For a given average number of particles per node ρ the nonlinear Boltzmann equation Eq. (16) has a spatially homogeneous stationary solution $f_i(\mathbf{r}) = f_{\mathrm{eq}} = \rho/b$, satisfying

$$\Omega^{10}(f_{\mathrm{eq}}) = 0. \tag{18}$$

B. The linearized Boltzmann equation

In a first attempt to understand the solutions to the Boltzmann equation Eq. (16) we study small deviations from equilibrium by linearizing around the equilibrium solution. Introducing the fluctuation $\delta f_i(\mathbf{r},t) = f_i(\mathbf{r},t) - f_{\mathrm{eq}}$ we have

$$\delta f_i(\mathbf{r}+\mathbf{c}_i,t+1)-\delta f_i(\mathbf{r},t)$$

$$=\sum_{\mathbf{r}'}\sum_j \left.\frac{\partial\Omega_i^{10}(\mathbf{r})}{\partial f_j(\mathbf{r}')}\right|_{\rm eq}\delta f_j(\mathbf{r}',t). \quad (19)$$

Since the outcome of a collision at node $\mathbf{r}$ only depends on the state of node $\mathbf{r}$ itself and of its nearest neighbors $\mathbf{r}+\mathbf{c}_p$ with $1\le p\le b$, the $\mathbf{r}'$ summation can be restricted to node $\mathbf{r}$ and its nearest neighbors. The resulting equation is the *linearized Boltzmann equation*

$$\delta f_i(\mathbf{r}+\mathbf{c}_i,t+1)-\delta f_i(\mathbf{r},t)=\sum_{p=0}^{b}\sum_j \Omega_{ij}^{11,p}\delta f_j(\mathbf{r}+\mathbf{c}_p,t), \quad (20)$$

where $\mathbf{c}_0=0$ by definition, and the linearized Boltzmann operator $\Omega_{ij}^{11,p}$ is defined as ($\delta s_i=s_i-f$)

$$\Omega_{ij}^{11,p}\equiv\left.\frac{\partial\Omega_i^{10}(\mathbf{r})}{\partial f_j(\mathbf{r}+\mathbf{c}_p)}\right|_{\rm eq}=\left\langle[\sigma_i(\mathbf{r})-s_i(\mathbf{r})]\frac{\delta s_j(\mathbf{r}+\mathbf{c}_p)}{g_{\rm eq}}\right\rangle_{\rm MF,eq}, \quad (21)$$

with the single particle fluctuation $g_{\rm eq}$ given by

$$g_{\rm eq}=f_{\rm eq}(1-f_{\rm eq}). \quad (22)$$

The second equality in Eq. (21) follows from the definition of $\langle\,\rangle_{\rm MF}$ in Eq. (14). The equilibrium average $\langle\,\rangle_{\rm MF,eq}$ is defined by Eq. (14) with $F(s,\mathbf{r},t)=F_{\rm eq}(s)$.

In Appendix A the symmetry properties of the matrices $\Omega^{11,p}$ are discussed. One result is that $\Omega_{ij}^{11,0}$ does not depend on β or $f_{\rm eq}$, and is given by

$$\Omega_{ij}^{11,0}=\frac{1}{b}-\delta_{ij}. \quad (23)$$

For $1\le p\le b$ the matrix $\Omega_{ij}^{11,p}$ does not depend on its second index j. Therefore it is convenient to define the symbol ω_i^p as

$$\omega_i^p\equiv\frac{1}{b}\sum_j\Omega_{ij}^{11,p}. \quad (24)$$

As is shown in Appendix A, on the square lattice ($b=4$) there are only two independent elements ω_1^1 and ω_2^1; all other ω_i^p are related to these two by lattice symmetries. On the half-filled square lattice ($f_{\rm eq}=\frac{1}{2}$) we have $\omega_2^1=0$. On the triangular lattice ($b=6$) only ω_1^1, ω_2^1, and ω_3^1 are independent, and when $f_{\rm eq}=\frac{1}{2}$ we have $\omega_3^1=-\omega_2^1$.

The linearized Boltzmann equation Eq. (20) represents a set of spatially coupled linear evolution equations for $f_i(\mathbf{r},t)$. A standard way of treating such equations is by means of Fourier transformation,

$$f_i(\mathbf{k},t)=\sum_{\mathbf{r}}e^{-i\mathbf{k}\cdot\mathbf{r}}\delta f_i(\mathbf{r},t). \quad (25)$$

Each Fourier component $\mathbf{k}$ evolves independently according to

$$f_i(\mathbf{k},t+1)=\sum_j\Gamma_{ij}^B(\mathbf{k})\delta f_j(\mathbf{k},t). \quad (26)$$

The one-step Boltzmann propagator $\Gamma_{ik}^B(\mathbf{k})$ is defined as

$$\Gamma_{ij}^B(\mathbf{k})=e^{-i\mathbf{k}\cdot\mathbf{c}_i}\left[\delta_{ij}+\sum_{p=0}^{b}e^{i\mathbf{k}\cdot\mathbf{c}_p}\,\Omega_{ij}^{11,p}\right]=e^{-i\mathbf{k}\cdot\mathbf{c}_i}\left[\frac{1}{b}+\sum_{p=1}^{b}e^{i\mathbf{k}\cdot\mathbf{c}_p}\,\omega_i^p\right], \quad (27)$$

where the second equality follows from Eqs. (23) and (24). The propagator is a nonsymmetric matrix. Introducing a bra-ket notation with left eigenvectors $\langle\tilde{\psi}_\mu(\mathbf{k})|$ and right eigenvectors $|\psi_\mu(\mathbf{k})\rangle$ corresponding to eigenvalue $e^{z_\mu(\mathbf{k})}$ we can write the propagator as a spectral decomposition

$$\Gamma_{ij}^B(\mathbf{k})=\sum_\mu|\psi_\mu(\mathbf{k})\rangle_i\,e^{z_\mu(\mathbf{k})}\,\langle\tilde{\psi}_\mu(\mathbf{k})|_j, \quad (28)$$

where μ runs over b different *modes*. The eigenvectors satisfy a biorthogonality relation

$$\langle\tilde{\psi}_\mu(\mathbf{k})|\psi_\nu(\mathbf{k})\rangle=\delta_{\mu\nu}, \quad (29)$$

where the inner product is defined by $\langle a|b\rangle=\sum_{i=1}^b a_ib_i$ (no complex conjugation).

Since the Boltzmann propagator $\Gamma_{ij}^B(\mathbf{k})$ does not depend on its second index (see Appendix A), the vector $(1,\ldots,1)$ necessarily is a left eigenvector; it is associated with a diffusive mode $\mu=$D. All other modes relax instantaneously, i.e., $e^{z_\mu(\mathbf{k})}=0$ for $\mu\ne$ D. This is due to the fact that the outcome of the collision step only depends on the densities $\rho(\mathbf{r}+\mathbf{c}_p)$ at the central node and its nearest neighbors; all other information about the precollision state is completely lost. Consequently $\Gamma_{ij}^B(\mathbf{k})$ has the structure of a projection operator,

$$\Gamma_{ij}^B(\mathbf{k})=|\psi_D(\mathbf{k})\rangle_i\,e^{z_D(\mathbf{k})}\,\langle\tilde{\psi}_D(\mathbf{k})|_j, \quad (30)$$

projecting onto the diffusive mode $\mu=$D associated with the locally conserved density.

It can be verified that for all $\mathbf{k}$ the left and right eigenvectors are given by

$$\langle\tilde{\psi}_D(\mathbf{k})|_i=1,$$

$$|\psi_D(\mathbf{k})\rangle_i=e^{-z_D(\mathbf{k})}\left\{e^{-i\mathbf{k}\cdot\mathbf{c}_i}\left(\frac{1}{b}+\sum_{p=1}^{b}e^{i\mathbf{k}\cdot\mathbf{c}_p}\,\omega_i^p\right)\right\}, \quad (31)$$

and the eigenvalue $e^{z_D(\mathbf{k})}$ by

$$z_D(\mathbf{k})=\ln\left\{\sum_{i=1}^{b}e^{-i\mathbf{k}\cdot\mathbf{c}_i}\left(\frac{1}{b}+\sum_{p=1}^{b}e^{i\mathbf{k}\cdot\mathbf{c}_p}\,\omega_i^p\right)\right\}. \quad (32)$$

For small values of the wave number $k=|\mathbf{k}|$ we can expand

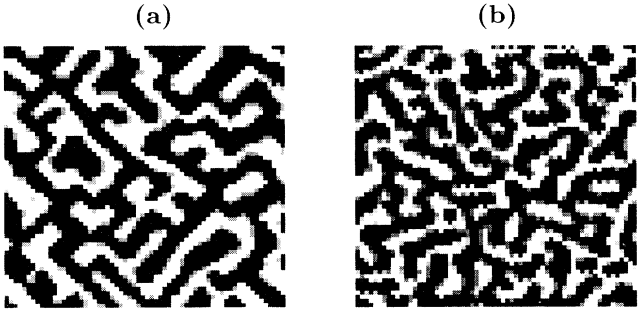

FIG. 1. Pattern formation for $\beta > \beta_c$ on (a) the square lattice, where there is a clear preference for $\pm 45°$ directions, and (b) the triangular lattice, where this anisotropy is absent.

$$z_D(\mathbf{k}) = -Dk^2 + O(k^4), \tag{33}$$

where the diffusion coefficient D is given by

$$D = \tfrac{1}{4} - \tfrac{1}{2} \sum_{i,p=1}^{b} (\mathbf{c}_i \cdot \mathbf{c}_p)\, \omega_i^p. \tag{34}$$

The sign of D determines whether the diffusive mode is stable ($D > 0$) or unstable ($D < 0$). Since the ω_i^p are functions of β, the condition $D(\beta_c) = 0$ defines a critical inverse temperature β_c.

C. Critical temperature and isotropy

On the square lattice where $b = 4$ we can use the symmetries of ω_i^p to obtain

$$\begin{aligned} z_D(\mathbf{k}) = \ln[&\tfrac{1}{2}(\cos k_x + \cos k_y) \\ &+4(\omega_1^1 + \omega_2^1)(\sin^2 k_x + \sin^2 k_y) \\ &-4\omega_2^1(\cos k_x - \cos k_y)^2], \end{aligned} \tag{35}$$

The diffusion coefficient is given by $D = \frac{1}{4} - 4(\omega_1^1 + \omega_2^1)$. In what follows we specialize to the case of the half-filled lattice $f = \frac{1}{2}$, where ω_2^1 vanishes, so that the condition $D(\beta_c) = 0$ is equivalent to $\omega_1^1(\beta_c) = \frac{1}{16}$. In Appendix B it is shown that a "high temperature expansion" yields $\omega_1^1(\beta) = \frac{1}{4}\beta + O(\beta^2)$. Therefore in first approximation $\beta_c = \frac{1}{4}$. A more precise (numerical) calculation yields $\beta_c \simeq 0.263$. In Ref. [17] it was found from computer simulations that β_c =0.30–0.35. The discrepancy between these simulation values and our theoretical prediction for β_c is due to the complete neglect of correlated fluctuations inherent in the Boltzmann approximation. In the next section we will present a systematic improvement of Boltzmann theory which takes some of the correlations into account.

Figure 1 shows snapshots of the time evolution of a system that at $t = 0$ is prepared in a spatially uniform initial state. The inverse temperature is chosen such that the model is spatially unstable: $\beta > \beta_c$. On the left hand side of Fig. 1 particles move on a square lattice; on the right hand side a triangular lattice is used. In the former case there clearly exists a strong preference for patterns in which angles of $\pm 45°$ with the x and y axes dominate. This anisotropy is absent on the triangular lattice.

Can Boltzmann theory predict such features of the patterns? That this is indeed the case is shown in Fig. 2 where the unstable regions with $z_D(\mathbf{k}) > 0$ are indicated in the $\mathbf{k}$ plane. In the case of the triangular lattice $z_D(\mathbf{k})$ hardly depends on the direction of $\mathbf{k}$. On the square lattice, however, there are four distinguished maxima located in the $\pm 45°$ directions. Analytical insight can be gained by expanding $z_D(\mathbf{k})$ in powers of the Cartesian components k_α of $\mathbf{k}$, with tensorial coefficients, as

$$z_D(\mathbf{k}) = -D_{\alpha\beta}k_\alpha k_\beta + E_{\alpha\beta\gamma\delta}k_\alpha k_\beta k_\gamma k_\delta + \cdots . \tag{36}$$

The second rank tensor $D_{\alpha\beta} = D\delta_{\alpha\beta}$ is isotropic on both the square and the triangular lattices. However, the fourth rank tensor $E_{\alpha\beta\gamma\delta}$ is isotropic on the triangular lattice only; on the square lattice it gives rise to anisotropic quartic terms k_α^4. When $D > 0$ the macro-

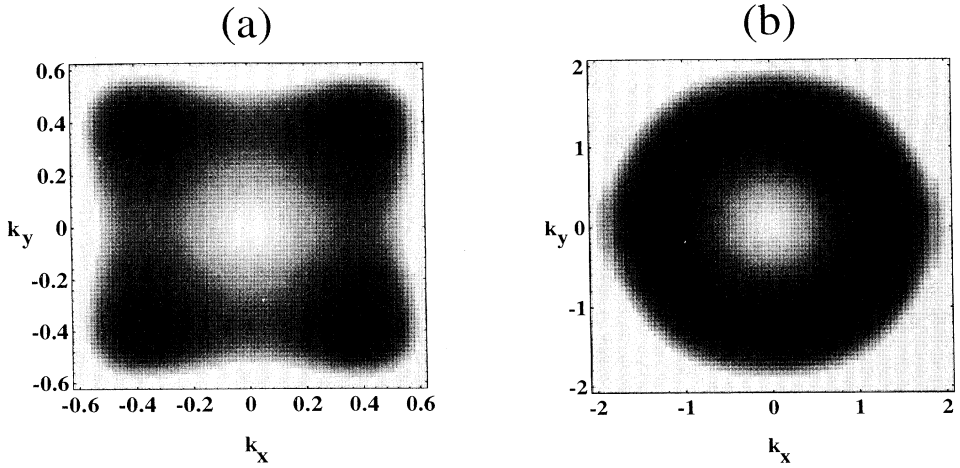

FIG. 2. Diffusive eigenvalue $z_D(\mathbf{k})$. Regions where $z_D(\mathbf{k}) > 0$ are indicated by gray scales: black denotes the fastest growing modes. (a) On the square lattice there exist strong anisotropies. (b) On the triangular lattice the spectrum is nearly isotropic.

scopic behavior of the model is dominated by the large wavelength modes around $\mathbf{k} = \mathbf{0}$. But in the case of spatial instability the fastest initial growth occurs at finite wave numbers, and therefore the higher order terms in Eq. (36) become important as well. Consequently the isotropic symmetry is absent in Fig. 2(a).

IV. DRIVEN DIFFUSION

The dynamics of the model can be modified by introducing an external driving field $\mathbf{E}$, extending the definition of the collision rules in Eq. (6) as follows:

$$A_{s\sigma}(\mathbf{G},\mathbf{E}) = \frac{1}{Z(s)} e^{(\beta\mathbf{G}+\mathbf{E})\cdot\mathbf{J}(\sigma)}\, \delta(\rho(\sigma),\rho(s)), \qquad (37)$$

with a normalization constant

$$Z(s) = \sum_{\sigma} e^{(\beta\mathbf{G}+\mathbf{E})\cdot\mathbf{J}(\sigma)}\, \delta(\rho(\sigma),\rho(s)). \qquad (38)$$

The driving field breaks the symmetry of the stationary solution to the nonlinear Boltzmann equation given by Eq. (18). It now has the form $f_i^{\mathrm{eq}}(\mathbf{r}) = f_i$, with f_i depending on the direction $\mathbf{c}_i$. Numerically, the stationary solution is obtained within a few iteration steps, by iterating $f_i \to f_i + \Omega_i^{10}(f_i)$, starting from $f_i = \rho/b$.

The driving field $\mathbf{E}$ induces a stationary average particle flux $\mathbf{J}_0$ throughout the lattice. In Fig. 3(a) $|\mathbf{J}_0|$ is plotted against $|\mathbf{E}|$, for two directions $\mathbf{E} \sim (1,0)$ and $\mathbf{E} \sim (1,1)$, respectively. There is good agreement between theory and simulations. Up to $|\mathbf{E}| \simeq 0.5$ the response is linear and isotropic, $\mathbf{J}_0 = \chi\mathbf{E}$ with $\chi = \chi(\beta, f_{\mathrm{eq}})$ the susceptibility. In Appendix C it is derived that in the mean-field approximation χ is given by a *linear response* relation in terms of the variance of the postcollision flux $\mathbf{J}(\sigma)$ in equilibrium,

$$\chi = \tfrac{1}{2}\left\langle \overline{\mathbf{J}^2(\sigma)} - \overline{\mathbf{J}(\sigma)}^2 \right\rangle_{\mathrm{MF,eq}}, \qquad (39)$$

with

$$\overline{\mathbf{J}(\sigma)} \equiv \sum_{\sigma} \mathbf{J}(\sigma) A_{s\sigma}(\mathbf{G}), \qquad \overline{\mathbf{J}^2(\sigma)} \equiv \sum_{\sigma} [\mathbf{J}(\sigma)]^2 A_{s\sigma}(\mathbf{G}). \qquad (40)$$

In the special case $\beta = 0$ the susceptibility is given by $\chi = \frac{1}{2} b g_{\mathrm{eq}}$, on both the square and the triangular lattices.

The spatial stability of the system in the presence of a driving field $\mathbf{E}$ can be determined by linearizing around the appropriate stationary state $f_i(\mathbf{r}) = f_i(\rho, \beta, \mathbf{E})$. The symmetries of $\Omega^{11,p}$ for $\mathbf{E} = \mathbf{0}$ that enabled us to calculate the eigenvalue spectrum $\{z_\mu(\mathbf{k})\}$ analytically are all lost due to the symmetry breaking driving field $\mathbf{E}$.

By observing the diffusion coefficient $D(\hat{\mathbf{k}}) = -\lim_{k\downarrow 0} z_D(\mathbf{k})/k^2$ as a function of the direction $\hat{\mathbf{k}} = \mathbf{k}/k$ we can monitor how the system becomes unstable as β increases from $\beta = 0$. In the preceding section we found that when $\mathbf{E} = \mathbf{0}$ all $\hat{\mathbf{k}}$ directions become unstable simultaneously at $\beta_c \simeq 0.263$. From Fig. 4 it can be seen that the external field suppresses the unstable fluctuations so that the critical value of β is increased to $\beta_{c,1}(\mathbf{E}) > \beta_c$. The suppression is most effective for excitations with $\mathbf{k}$ parallel to $\mathbf{E}$ so that those with $\mathbf{k} \perp \mathbf{E}$ are the first to become unstable for $\beta > \beta_{c,1}(\mathbf{E})$, which results in the emergence of a striped phase. When the temperature is further decreased, the range of unstable $\hat{\mathbf{k}}$ directions

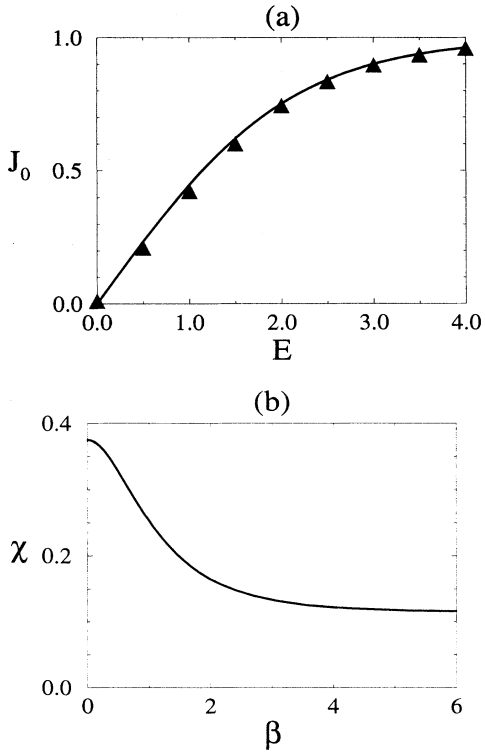

FIG. 3. Square lattice model at $f_{\mathrm{eq}} = \frac{1}{2}$. (a) Average induced particle flux J_0 versus driving field E, with $\mathbf{E} \sim \hat{\mathbf{x}}$. The solid lines represent mean-field theory; simulation results are shown as symbols. (b) Susceptibility χ versus β.

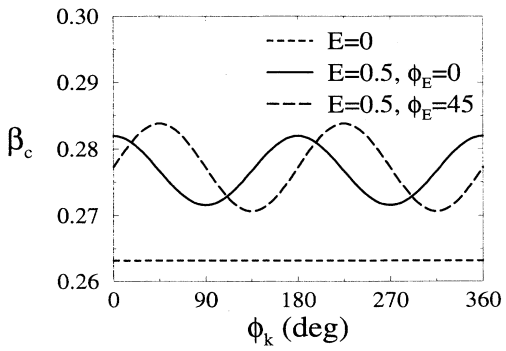

FIG. 4. Critical temperature $T_c(\hat{\mathbf{k}}, \mathbf{E})$ versus ϕ_k, the angle of $\hat{\mathbf{k}}$ with the positive x axis, for the negative diffusion model on the half-filled square lattice ($f_{\mathrm{eq}} = \frac{1}{2}$), in the presence of an external driving field $\mathbf{E}$, with strength $|\mathbf{E}| = \frac{1}{2}$ and direction $\mathbf{E} \sim (1,0)$ or $\mathbf{E} \sim (1,1)$.

spreads out until at $\beta = \beta_{c,2}(\mathbf{E})$ the spectrum $z_D(\mathbf{k})$ has become unstable in all $\mathbf{k}$ directions. For still larger values of β the influence of $\mathbf{E}$ becomes negligible because $\beta\mathbf{G}$ dominates the term $(\beta\mathbf{G} + \mathbf{E})$ in Eq. (37), so that the patterns occurring are similar to those in Fig. 1 again.

A remark should be made about the kinetic eigenvalues $z_\mu(\mathbf{k})$ with $\mu \neq D$. In the previous section when discussing the case $\mathbf{E} = \mathbf{0}$ we argued that apart from the diffusive mode $z_D(\mathbf{k})$ there are three kinetic modes which decay to zero in a single evolution step. In the presence of a driving field $\mathbf{E} \neq \mathbf{0}$ these modes have a finite lifetime, i.e., $e^{z_\mu} \neq 0$. As long as the kinetic modes decay rapidly with respect to the (slow) diffusive mode, i.e., $z_\mu(\mathbf{k})/z_D(\mathbf{k}) \gg 1$, at least for small $\mathbf{k}$, the macroscopic evolution of the density field $\rho(\mathbf{r})$ is well described by the information contained in $z_D(\mathbf{k})$ only. This is the case for driving fields up to $|\mathbf{E}| \simeq 1$. For still larger values of $|\mathbf{E}|$ the value of the kinetic eigenvalues becomes comparable to $z_D(\mathbf{k})$ even near $\mathbf{k} = \mathbf{0}$, and they may even become positive. Clearly then our analysis in terms of the diffusive mode only is no longer adequate.

Keeping the above proviso in mind we can explain some observations made by Alexander *et al.* [17]. These authors report on the occurrence of a striped phase as the temperature is decreased below a critical value, with structure perpendicular to a driving field $\mathbf{E}$. Furthermore, they mention that there also appears to be a second transition at a lower temperature to a phase with structures resembling those found for $\mathbf{E} = \mathbf{0}$. Unfortunately the authors used $\mathbf{E} = (4, 0)$ and as was argued above our theory breaks down at such a large value of $|\mathbf{E}|$. However, qualitatively at least, the observations of Alexander *et al.* are consistent with our findings for $\mathbf{E} = (\frac{1}{2}, 0)$.

V. ENSKOG THEORY

A. Equilibrium correlations

In this section we extend the theory of Ref. [10] to the model considered in this article. Here we will follow a more intuitive line of argument which, however, leads to the same results. For a more systematic derivation of the results of this section we refer to Ref. [10].

The leading term describing the deviation from the completely factorized distribution — which is characterized by the single particle distribution function $f_i(\mathbf{r}, t)$ — is the pair correlation function $G_{ij}(\mathbf{r}, \mathbf{r}', t)$ defined by

$$G_{ij}(\mathbf{r}, \mathbf{r}', t) = \langle \delta s_i(\mathbf{r}, t) \delta s_j(\mathbf{r}', t) \rangle$$

$$= \langle s_i(\mathbf{r}, t) s_j(\mathbf{r}', t) \rangle - f_i(\mathbf{r}, t) f_j(\mathbf{r}', t). \quad (41)$$

Note that the diagonal elements are not independent since

$$G_{ii}(\mathbf{r}, \mathbf{r}, t) = f_i(\mathbf{r}, t)[1 - f_i(\mathbf{r}, t)]. \quad (42)$$

In what follows we assume that the system is spatially homogeneous in a statistical sense, so that $f_i(\mathbf{r}) = f = \rho/b$ and

$$G_{ij}(\mathbf{r}, \mathbf{r}', t) = \mathcal{G}_{ij}(\mathbf{r} - \mathbf{r}', t). \quad (43)$$

It is convenient to introduce the *excess correlation function* $\mathcal{C}_{ij}(\mathbf{r}, t)$, defined as

$$\mathcal{C}_{ij}(\mathbf{r}, t) = \mathcal{G}_{ij}(\mathbf{r}, t) - \delta(\mathbf{r}) \delta_{ij} g_{\text{eq}}. \quad (44)$$

In this section we will formulate a kinetic theory beyond the Boltzmann approximation that makes use of a refined description of the phase space distribution function by taking into account both $f_i(\mathbf{r}, t)$ and $\mathcal{G}_{ij}(\mathbf{r}, t)$. Three-point and higher order correlation functions are still neglected. In the next section we will explain how this extension gives rise to corrections to the Boltzmann theory for the diffusion coefficient $D(\beta)$ and the critical inverse temperature β_c. But first we will describe how the pair correlation function in equilibrium $\mathcal{G}_{ij}^{\text{eq}}(\mathbf{r})$ can be calculated, at least approximately.

The reason for the existence of static (equal time) correlations between fluctuations $\delta s_i(\mathbf{r}, t)$ is that the collision rules violate detailed balance: there does not exist a completely factorized equilibrium distribution that is invariant under the combined action of the collision and the propagation step. To see this explicitly we consider the source term $B_{ij}(\mathbf{r} - \mathbf{r}')$, representing the *postcollision* pair correlations that are created when the collision rules are applied to a completely factorized *precollision* state,

$$B_{ij}(\mathbf{r} - \mathbf{r}') \equiv \langle \delta\sigma_i(\mathbf{r}) \delta\sigma_j(\mathbf{r}') - \delta s_i(\mathbf{r}) \delta s_j(\mathbf{r}') \rangle_{\text{MF,eq}}$$
$$= [1 - \delta_{ij} \delta(\mathbf{r}, \mathbf{r}')] \langle \delta\sigma_i(\mathbf{r}) \delta\sigma_j(\mathbf{r}') \rangle_{\text{MF,eq}}. \quad (45)$$

The second equality follows from $\langle [\delta\sigma_i(\mathbf{r})]^2 \rangle = \langle \delta(s_i(\mathbf{r}))^2 \rangle = g_{\text{eq}}$.

It follows from the definition of the collision rules that $B_{ij}(\mathbf{r} - \mathbf{r}')$ can only be nonvanishing if $\mathbf{r}$ and $\mathbf{r}'$ have at least one nearest neighbor in common. Splitting $B_{ij}(\mathbf{r})$ into contributions of four different types we have

$$B_{ij}(\mathbf{r}) = \delta(\mathbf{r}) \Omega_{ij}^{20}(\mathbf{0}) + \sum_{p=1}^{b} [\delta(\mathbf{r}, \mathbf{c}_p) \Omega_{ij}^{20}(\mathbf{c}_p)$$
$$+ \delta(\mathbf{r}, 2\mathbf{c}_p) \Omega_{ij}^{20}(2\mathbf{c}_p)$$
$$+ \delta(\mathbf{r}, \mathbf{c}_p + \mathbf{c}_{p+1}) \Omega_{ij}^{20}(\mathbf{c}_p + \mathbf{c}_{p+1})]. \quad (46)$$

The matrices $\Omega_{ij}^{20}(\mathbf{r})$ are defined by

$$\Omega_{ij}^{20}(\mathbf{r}) = \langle \delta\sigma_i(\mathbf{r}) \delta\sigma_j(\mathbf{0}) \rangle_{\text{MF,eq}}$$
$$= \sum_{s(\mathbf{r})} \sum_{\sigma(\mathbf{r})} \delta\sigma_i(\mathbf{r}) \delta\sigma_j(\mathbf{0})$$
$$\times \prod_{\mathbf{r}} \left[A_{s(\mathbf{r}),\sigma(\mathbf{r})}(\mathbf{G}(\mathbf{r})) F(s(\mathbf{r})) \right], \quad (47)$$

with $\Omega_{ii}^{20}(\mathbf{0}) = 0$ by definition. Introducing the Fourier transforms of $\mathcal{C}_{ij}(\mathbf{r})$ and $B_{ij}(\mathbf{r})$,

$$\hat{\mathcal{C}}_{ij}(\mathbf{q}) = \sum_{\mathbf{r}} e^{-i\mathbf{q}\cdot\mathbf{r}} \mathcal{C}_{ij}(\mathbf{r}), \qquad \hat{B}_{ij}(\mathbf{q}) = \sum_{\mathbf{r}} e^{-i\mathbf{q}\cdot\mathbf{r}} B_{ij}(\mathbf{r}), \quad (48)$$

we write Eq. (46) as

$$\hat{B}_{ij}(\mathbf{q}) = \Omega_{ij}^{20}(\mathbf{0}) + \sum_{p=1}^{b}[e^{-i\mathbf{q}\cdot\mathbf{c}_p}\Omega_{ij}^{20}(\mathbf{c}_p) + e^{-2i\mathbf{q}\cdot\mathbf{c}_p}\Omega_{ij}^{20}(2\mathbf{c}_p) + e^{-i\mathbf{q}\cdot(\mathbf{c}_p+\mathbf{c}_{p+1})}\Omega_{ij}^{20}(\mathbf{c}_p+\mathbf{c}_{p+1})]. \quad (49)$$

Within the approximation that is used here we may consider the correlations that result from sources at different times to evolve independently (this is the "simple ring approximation" of Ref. [10], in which repeated rings and higher order correlated collisions have been neglected). Let us first turn to the question how the correlations that are generated by the source term at time t_0 evolve in time. We start by observing that the propagation step transforms the postcollision correlations created by B_{ij} at time t_0 into precollision correlations at time t_0+1, according to

$$\hat{C}_{ij}(\mathbf{q}, t_0+1|t_0) = S_i(\mathbf{q})S_j(-\mathbf{q})B_{ij}(\mathbf{q}|t_0), \quad (50)$$

with the streaming operator in Fourier representation given by

$$S_i(\mathbf{q}) \equiv e^{-i\mathbf{q}\cdot\mathbf{c}_i}. \quad (51)$$

In Eq. (50) we have used t_0 as a label, indicating that $\hat{C}_{ij}(\mathbf{q}, t|t_0)$ contains the contribution to $\hat{C}_{ij}(\mathbf{q}, t)$ of correlations that are created by the source term $\hat{B}_{ij}(\mathbf{q})$ at time t_0 *only*. In the simple ring approximation the fluctuations $\delta s_i(\mathbf{q}, t|t_0)$ in

$$\hat{C}_{ij}(\mathbf{q}, t|t_0) = \langle \delta s_i(\mathbf{q}, t|t_0)\delta s_j(-\mathbf{q}, t|t_0)\rangle, \quad (52)$$

which are initially correlated at t_0, evolve independently according to

$$\delta s_i(\mathbf{q}, t+1|t_0) = \sum_{k=1}^{b}\Gamma_{ik}(\mathbf{q})\delta s_k(\mathbf{q}, t|t_0). \quad (53)$$

The $\mathbf{q}$-dependent $b \times b$ matrix $\Gamma_{ik}(\mathbf{q})$ is the single particle one-step propagator. In Sec. V C we will derive an extension of the linearized Boltzmann equation — the linear Enskog equation — which takes the static equilibrium correlations $\mathcal{C}_{ij}^{\mathrm{eq}}(\mathbf{r})$ into account. The corresponding *Enskog propagator* $\Gamma_{ik}^{E}(\mathbf{q})$ describes the time evolution of a single fluctuation in the correlated background of all other particles. In Sec. V D we will argue that for a self-consistent theory it is required that we take $\Gamma_{ik}(\mathbf{q}) = \Gamma_{ik}^{E}(\mathbf{q})$ in Eq. (53).

Combining Eqs. (50), (52), and (53) we obtain

$$\begin{aligned}\hat{C}(\mathbf{q}, t|t_0) &= \sum_{k,\ell=1}^{b}\Gamma_{ik}^{t-t_0-1}(\mathbf{q})\Gamma_{j\ell}^{t-t_0-1}(-\mathbf{q})\hat{C}_{k\ell}(\mathbf{q}, t_0+1|t_0) \\ &= \sum_{k,\ell=1}^{b}\Gamma_{ik}^{t-t_0-1}(\mathbf{q})\Gamma_{j\ell}^{t-t_0-1}(-\mathbf{q}) \\ &\quad \times S_k(\mathbf{q})S_\ell(-\mathbf{q})\hat{B}_{k\ell}(\mathbf{q}|t_0). \end{aligned} \quad (54)$$

In equilibrium the correlations $\hat{C}_{ij}^{\mathrm{eq}}(\mathbf{q})$ at time t are given by a superposition of contributions from sources at all previous times $t_0 < t$ that all evolve independently,

$$\hat{C}_{ij}^{\mathrm{eq}}(\mathbf{q}) = \sum_{t_0=-\infty}^{t-1}\hat{C}_{ij}(\mathbf{q}, t|t_0). \quad (55)$$

Inserting Eq. (54) into Eq. (55) we arrive at the following expression for the pair correlations in equilibrium, calculated in the simple ring approximation:

$$\hat{C}_{ij}(\mathbf{q}) = \sum_{k,\ell}\left[\frac{1}{1-\Gamma(\mathbf{q})\Gamma(-\mathbf{q})}\right]_{ij,k\ell}S_k(\mathbf{q})S_\ell(-\mathbf{q})\hat{B}_{k\ell}(\mathbf{q}). \quad (56)$$

Finally we calculate $\mathcal{C}_{ij}^{\mathrm{eq}}(\mathbf{r})$ using the inverse Fourier transformation,

$$\mathcal{C}_{ij}^{\mathrm{eq}}(\mathbf{r}) = \frac{1}{V}\sum_{\mathbf{q}}e^{i\mathbf{q}\cdot\mathbf{r}}\hat{\mathcal{C}}_{ij}^{\mathrm{eq}}(\mathbf{q}), \quad (57)$$

where $\mathbf{q}$ runs over the first Brillouin zone.

B. The Enskog equation

In Sec. III we have derived the linearized Boltzmann equation Eq. (20) by assuming a completely factorized distribution over phase space according to Eq. (13). We will now extend the Boltzmann equation by taking into account the effect of the static pair correlations $\mathcal{G}_{ij}^{\mathrm{eq}}(\mathbf{r}-\mathbf{r}')$ calculated in the previous section. In the spirit of the Enskog theory for hard spheres [18] we modify the *Stosszahlansatz* by taking pair correlations into account in the collision term Eq. (12). We start from the following identity, valid for Boolean variables:

$$\begin{aligned}\delta(s_i(\mathbf{r}, t), n_i(\mathbf{r}, t)) &= n_i(\mathbf{r}, t)^{s_i(\mathbf{r})}[1-n_i(\mathbf{r}, t)]^{1-s_i(\mathbf{r})} \\ &= [f_{\mathrm{eq}}+\delta n_i(\mathbf{r}, t)]^{s_i(\mathbf{r})}[1-f_{\mathrm{eq}}-\delta n_i(\mathbf{r}, t)]^{1-s_i(\mathbf{r})} \\ &= f_{\mathrm{eq}}^{s_i(\mathbf{r})}(1-f_{\mathrm{eq}})^{1-s_i(\mathbf{r})}\left(1+\frac{\delta s_i(\mathbf{r})\delta n_i(\mathbf{r}, t)}{g_{\mathrm{eq}}}\right). \end{aligned} \quad (58)$$

Here $\delta s_i(\mathbf{r},t) = s_i(\mathbf{r},t) - f_{\rm eq}$ and $\delta n_i(\mathbf{r},t) = n_i(\mathbf{r},t) - f_{\rm eq}$ are fluctuations with respect to equilibrium. From Eqs. (9) and (58) we obtain

$$p(\{s(\mathbf{r})\},t) = \left(\prod_{\mathbf{r}} F_{\rm eq}(s(\mathbf{r}))\right) \times \left\langle \prod_{\mathbf{r},i}\left(1 + \frac{\delta s_i(\mathbf{r})\delta n_i(\mathbf{r},t)}{g_{\rm eq}}\right)\right\rangle, \quad (59)$$

where the angular brackets still represent an average over a *nonequilibrium* initial state. Now consider a nonequilibrium ensemble describing a small deviation from the equilibrium state. For the single particle fluctuation we have

$$\langle \delta n_i(\mathbf{r},t)\rangle = f_i(\mathbf{r},t) - f_{\rm eq} = \delta f_i(\mathbf{r},t). \quad (60)$$

We assume that close to equilibrium we may approximate the pair correlation function by its equilibrium value, i.e.,

$$\langle \delta n_i(\mathbf{r},t)\delta n_j(\mathbf{r}',t)\rangle \simeq \langle \delta n_i(\mathbf{r},t)\delta n_j(\mathbf{r}',t)\rangle_{\rm eq} \equiv \mathcal{G}^{\rm eq}_{ij}(\mathbf{r}-\mathbf{r}'), \quad (61)$$

with $\mathcal{G}^{\rm eq}_{ij}(\mathbf{r}-\mathbf{r}')$ given by the theory of Sec. III A. To obtain a closed time evolution equation for $\delta f_i(\mathbf{r},t)$ we systematically expand the average in Eq. (59) up to third order in the fluctuations,

$$\left\langle \prod_{\mathbf{r},i}\left(1 + \frac{\delta s_i(\mathbf{r})\delta n_i(\mathbf{r},t)}{g_{\rm eq}}\right)\right\rangle$$

$$\simeq 1 + \sum_{\mathbf{r},i}\frac{\delta s_i(\mathbf{r})}{g_{\rm eq}}\langle \delta n_i(\mathbf{r},t)\rangle + \sum_{(\mathbf{r},k)<(\mathbf{r}',\ell)}\frac{\delta s_k(\mathbf{r})}{g_{\rm eq}}\frac{\delta s_\ell(\mathbf{r}')}{g_{\rm eq}}\langle \delta n_k(\mathbf{r},t)\delta n_\ell(\mathbf{r}',t)\rangle + \sum_{(\mathbf{r},k)<(\mathbf{r}',\ell)<(\mathbf{r}'',m)}\frac{\delta s_k(\mathbf{r})}{g_{\rm eq}}\frac{\delta s_\ell(\mathbf{r}')}{g_{\rm eq}}\frac{\delta s_m(\mathbf{r}'')}{g_{\rm eq}}\langle \delta n_k(\mathbf{r},t)\delta n_\ell(\mathbf{r}',t)\delta n_m(\mathbf{r}'',t)\rangle, \quad (62)$$

where the sums run over all pairs and triplets of channels.

The three-point function occurring in Eq. (62) can be expanded in cluster functions as

$$\langle \delta n_k(\mathbf{r},t)\delta n_\ell(\mathbf{r}')\delta n_m(\mathbf{r}'')\rangle = \delta f_k(\mathbf{r},t)\delta f_\ell(\mathbf{r}',t)\delta f_m(\mathbf{r}'',t) + \delta f_k(\mathbf{r},t)G_{\ell m}(\mathbf{r}',\mathbf{r}'',t) + \delta f_\ell(\mathbf{r}',t)G_{km}(\mathbf{r},\mathbf{r}'',t) + \delta f_m(\mathbf{r}'',t)G_{k\ell}(\mathbf{r},\mathbf{r}',t) + G^{(3)}_{k\ell m}(\mathbf{r},\mathbf{r}',\mathbf{r}'',t). \quad (63)$$

We proceed by neglecting the three-particle cluster function $G^{(3)}$ and approximating the two-particle cluster function or pair correlation function $G_{k\ell}(\mathbf{r},\mathbf{r}')$ by its equilibrium value $\mathcal{G}^{\rm eq}_{k\ell}(\mathbf{r}-\mathbf{r}')$. By neglecting the term $O(\delta f^3)$ we arrive at the following expression:

$$\langle \delta n_k(\mathbf{r},t)\delta n_\ell(\mathbf{r}',t)\delta n_m(\mathbf{r}'',t)\rangle \simeq \delta f_k(\mathbf{r},t)\mathcal{G}^{\rm eq}_{\ell m}(\mathbf{r}'-\mathbf{r}'') + \delta f_\ell(\mathbf{r}',t)\mathcal{G}^{\rm eq}_{km}(\mathbf{r}-\mathbf{r}'') + \delta f_m(\mathbf{r}'',t)\mathcal{G}^{\rm eq}_{k\ell}(\mathbf{r}-\mathbf{r}'). \quad (64)$$

Putting Eqs. (59)–(64) together, we can evaluate the collision term in

$$\delta f_i(\mathbf{r}+\mathbf{c}_i,t+1) - \delta f_i(\mathbf{r},t) = \langle \sigma_i(\mathbf{r},t) - s_i(\mathbf{r},t)\rangle, \quad (65)$$

and obtain the linear *Enskog equation*,

$$\delta f_i(\mathbf{r}+\mathbf{c}_i,t+1) - \delta f_i(\mathbf{r},t) = \sum_{\mathbf{r}',j}\Omega^{11}_{ij}(\mathbf{r},\mathbf{r}')\delta f_j(\mathbf{r}',t) + \sum_{\mathbf{r}',j}\sum_{(\mathbf{r}'',k)<(\mathbf{r}''',\ell)}\Omega^{13}_{i,jk\ell}(\mathbf{r},\mathbf{r}',\mathbf{r}'',\mathbf{r}''') \times \mathcal{G}_{k\ell}(\mathbf{r}''-\mathbf{r}''')\delta f_j(\mathbf{r}',t). \quad (66)$$

The linear Boltzmann collision operator $\Omega^{11}_{ij}(\mathbf{r},\mathbf{r}')$ is given by

$$\Omega^{11}_{ij}(\mathbf{r},\mathbf{r}') = \left\langle [\sigma_i(\mathbf{r}) - s_i(\mathbf{r})]\frac{\delta s_j(\mathbf{r}')}{g_{\rm eq}}\right\rangle_{\rm MF,eq}. \quad (67)$$

The Enskog operator $\Omega^{13}_{i,k\ell m}(\mathbf{r},\mathbf{r}',\mathbf{r}'',\mathbf{r}''')$ vanishes by definition if two or more channels out of $(\mathbf{r}',\mathbf{c}_k)$, $(\mathbf{r}'',\mathbf{c}_\ell)$, and $(\mathbf{r}''',\mathbf{c}_m)$ are equal and is otherwise given by

$$\Omega^{13}_{i,jk\ell}(\mathbf{r},\mathbf{r}',\mathbf{r}'',\mathbf{r}''') = \left\langle [\sigma_i(\mathbf{r}) - s_i(\mathbf{r})] \frac{\delta s_j(\mathbf{r}')}{g_{\rm eq}} \frac{\delta s_k(\mathbf{r}'')}{g_{\rm eq}} \frac{\delta s_\ell(\mathbf{r}''')}{g_{\rm eq}} \right\rangle_{\rm MF,eq} . \tag{68}$$

Note that the first and third terms on the right hand side in Eq. (62) do not contribute to Eq. (66). This is a consequence of the conservation of particle number Eq. (3) together with rotational symmetry in the stationary state.

C. The Enskog propagator

In this section we work out the linear Enskog equation Eq. (66) for the model of Sec. II. Identification of Eqs. (21) and (67) allows us to write

$$\sum_{\mathbf{r}',j} \Omega^{11}_{ij}(\mathbf{r},\mathbf{r}')\delta f_j(\mathbf{r}',t) = \sum_{p=0}^{b} \sum_j \Omega^{11,p}_{ij} \delta f_j(\mathbf{r}+\mathbf{c}_p,t), \tag{69}$$

with $\Omega^{11,p}_{ij}$ defined in Eq. (21). Next we note that Eq. (68) can only be nonvanishing if all three nodes $\mathbf{r}'$, $\mathbf{r}'$, and $\mathbf{r}'''$ are either equal to $\mathbf{r}$ or a nearest neighbor of $\mathbf{r}$. Distinguishing different possibilities for the pair of channels $\{(\mathbf{r}'',\mathbf{c}_k),(\mathbf{r}''',\mathbf{c}_\ell)\}$ in the second term on the right hand side of Eq. (66) we obtain

$$\begin{aligned}
&\sum_{\mathbf{r}',j} \sum_{(\mathbf{r}'',k)<(\mathbf{r}''',\ell)} \Omega^{13}_{i,jk\ell}(\mathbf{r},\mathbf{r}',\mathbf{r}'',\mathbf{r}''')\mathcal{G}_{k\ell}(\mathbf{r}''-\mathbf{r}''')\delta f_j(\mathbf{r}',t) \\
&= \sum_{p=0}^{b}\sum_j \left\{ \sum_{q=0}^{b}\sum_{k<l} \Omega^{13,pqq}_{i,jk\ell}\mathcal{G}_{k\ell}(\mathbf{0}) + \sum_{q=0}^{b}\sum_{k,l} \Omega^{13,pq0}_{i,jk\ell}\mathcal{G}_{k\ell}(\mathbf{c}_q) + \sum_{q=0}^{b}\sum_{r=q+1}^{b}\sum_{k,l} \Omega^{13,pqr}_{i,jk\ell}\mathcal{G}_{k\ell}(\mathbf{c}_q-\mathbf{c}_r) \right\} \delta f_j(\mathbf{r}+\mathbf{c}_p,t) \\
&\equiv \sum_{p=0}^{b}\sum_j \overline{\Omega}^{13,p}_{ij}\delta f_j(\mathbf{r}+\mathbf{c}_p,t),
\end{aligned} \tag{70}$$

with

$$\Omega^{13,pqr}_{i,jk\ell} = \left\langle [\sigma_i(\mathbf{r}) - s_i(\mathbf{r})] \times \frac{\delta s_j(\mathbf{r}+\mathbf{c}_p)}{g_{\rm eq}} \frac{\delta s_k(\mathbf{r}+\mathbf{c}_q)}{g_{\rm eq}} \frac{\delta s_\ell(\mathbf{r}+\mathbf{c}_r)}{g_{\rm eq}} \right\rangle_{\rm MF,eq} . \tag{71}$$

In a manner completely analogous to Sec. III B we then obtain the time evolution equation for the Fourier component $f_i(\mathbf{k},t)$ defined in Eq. (25),

$$f_i(\mathbf{k},t+1) = \sum_{j=1}^{b} \Gamma^E_{ij}(\mathbf{k})\delta f_j(\mathbf{k},t). \tag{72}$$

The *Enskog propagator* $\Gamma^E_{ij}(\mathbf{k})$ is given by

$$\Gamma^E_{ij}(\mathbf{k}) = e^{-i\mathbf{k}\cdot\mathbf{c}_i} \left[\delta_{ij} + \sum_{p=0}^{b} e^{i\mathbf{k}\cdot\mathbf{c}_p} \left(\Omega^{11,p}_{ij} + \overline{\Omega}^{13,p}_{ij} \right) \right], \tag{73}$$

where Ω^{11}_{ij} is the linearized Boltzmann operator and $\overline{\Omega}^{13,p}_{ij}$ defined in Eq. (70) contains all terms depending on the equilibrium correlations $\mathcal{G}^{\rm eq}_{ij}(\mathbf{r})$.

Again we can write $\Gamma^E_{ij}(\mathbf{k})$ as a spectral decomposition,

$$\Gamma^E_{ij}(\mathbf{k}) = \sum_\mu |\psi_\mu(\mathbf{k})\rangle_i \, e^{z_\mu(\mathbf{k})} \, \langle\tilde{\psi}_\mu(\mathbf{k})|_j, \tag{74}$$

an important difference from the Boltzmann case being that now the $(b-1)$ kinetic modes $\mu \neq \text{D}$ have a finite relaxation time, i.e., $e^{z_\mu(\mathbf{k})} \neq 0$. The value of the Enskog diffusion coefficient $D_E(\beta)$ again follows from the small k behavior of the diffusive eigenvalue $z_D(\mathbf{k})$, as

$$D_E = -\lim_{\mathbf{k}\to 0} \frac{z_D(\mathbf{k})}{k^2}, \tag{75}$$

and can be evaluated either numerically or analytically by means of perturbation theory.

D. Self-consistent numerical evaluation

In the preceding sections we have explained (i) how the equilibrium correlations $\mathcal{G}^{\rm eq}_{ij}(\mathbf{r}-\mathbf{r}')$ can be calculated once the Enskog propagator $\Gamma^E_{ik}(\mathbf{q})$ is known, and (ii) how the Enskog propagator $\Gamma^E_{ik}(\mathbf{q})$ can be calculated once the equilibrium correlations $\mathcal{G}^{\rm eq}_{ij}(\mathbf{r}-\mathbf{r}')$ are known. For given density $f_{\rm eq} = \rho/b$ and inverse temperature β a self-consistent solution to Eq. (73) combined with Eqs. (56) and (57) can be obtained by iterating according to the following scheme.

(1) Calculate the source term $\hat{B}_{ij}(\mathbf{q})$ in Eq. (49) for given density $f_{\rm eq}$; this step needs to be performed only once since $\hat{B}_{ij}(\mathbf{q})$ is independent of $\mathcal{G}^{\rm eq}_{ij}(\mathbf{r}-\mathbf{r}')$.

(2) Assume that all pair correlations vanish, $\mathcal{G}^{\rm eq}_{ij}(\mathbf{r}-\mathbf{r}')=0$, so that the Enskog propagator $\Gamma^E_{ik}(\mathbf{q})$ in Eq. (73) reduces to the Boltzmann propagator $\Gamma^B_{ik}(\mathbf{q})$ given by Eq. (27).

(3) Calculate the pair correlations $\mathcal{G}^{\rm eq}_{ij}(\mathbf{r}-\mathbf{r}')$ using Eqs. (56) and (57) with the Enskog propagator $\Gamma^E_{ik}(\mathbf{q})$ obtained in the previous step.

(4) Calculate the Enskog propagator $\Gamma^E_{ik}(\mathbf{q})$ using Eqs. (70) and (73) with the pair correlations $\mathcal{G}^{\rm eq}_{ij}(\mathbf{r}-\mathbf{r}')$ obtained in the previous step.

(5) Repeat steps 3 and 4 until the scheme has converged; subsequently calculate the diffusion coefficient $D_E(\beta, f_{\rm eq})$ using Eq. (75).

This procedure works well for small values of β where the *Boltzmann* diffusion coefficient $D_B > 0$, so that $\|\Gamma^B(\mathbf{q})\| = |e^{z_D(\mathbf{q})}| < 1$. However, for $\beta > \beta_c(\text{Boltzmann}) \simeq 0.263$ we have $D_B < 0$. Consequently, $\|\Gamma^B(\mathbf{q})\| > 1$ for certain values of $|\mathbf{q}|$, and the infinite sum in Eq. (55) no longer converges. Thus step 3 cannot be performed after step 2 for $\beta > \beta_c(\text{Boltzmann})$.

There is a way out of this difficulty, since the static correlations that occur for $\beta \neq 0$ have the effect of *stabilizing* the system with respect to the Boltzmann case, i.e., $D_E(\beta) > D_{\rm B}(\beta)$. This enables us to extend the theory to values of β beyond $\beta_c(\text{Boltzmann})$ by a slight modification of the iterative scheme discussed above. We start from the self-consistent solution for some $\beta < \beta_c(\text{Boltzmann})$. Next we increase β by a small amount $\Delta\beta$ (typically ~ 0.01). After calculating the new source term according to step 1, we skip step 2. Instead the converged result for $\mathcal{G}^{\rm eq}_{ij}(\mathbf{r}-\mathbf{r}')$ corresponding to the old β value is used as the initial guess. Subsequent iteration of steps 3 and 4 then yields the new value of the diffusion coefficient at $\beta+\Delta\beta$. The procedure is extended by repeatedly increasing β by $\Delta\beta$ so that we can "adiabatically" follow $D_E(\beta)$ beyond $\beta = \beta_c(\text{Boltzmann})$.

Figure 5(a) shows the Boltzmann and Enskog diffusion coefficients D_B and D_E at density $f_{\rm eq} = \frac{1}{2}$, and as a function of β. These theoretical values are compared with simulation results $D_{\rm sim}$. The value of $D_{\rm sim}$ was measured by preparing a sinusoidal density perturbation at $t=0$, given by

$$f_i(\mathbf{r}, t=0) = f_{\rm eq} + \Delta f \sin(\mathbf{k}\cdot\mathbf{r}), \tag{76}$$

at a wave vector $\mathbf{k} = (2\pi/L, 0)$ along the x axis, and by subsequently identifying the diffusive decay of the Fourier component $\rho(\mathbf{k},t) = \sum_i f_i(\mathbf{k},t)$ according to $\rho(\mathbf{k},t) \sim \exp(-Dk^2t)$ with D the diffusion coefficient. During the first time step the decay is correctly described by the Boltzmann equation, since the initial state does not contain any correlations between fluctuations with respect to Eq. (76). But very soon correlations build up in the system, until at $t \simeq 50$ they have reached their stationary value $\mathcal{G}^{\rm eq}_{ij}(\mathbf{r}-\mathbf{r}')$. The decay of the density perturbation in this correlated background is slower than the initial decay. This is nicely illustrated by Fig. 5(b) showing $\rho(\mathbf{k},t)$ for $\beta = 0.30$ just above $\beta_c(\text{Boltzmann})$ where $D_B(\beta) < 0$ so that the density perturbation becomes unstable: it grows in time. As t increases the correlations lead to an increase of D and since β is not too far beyond $\beta_c(\text{Boltzmann})$ they change the sign of D from negative to positive, thus making the perturbation stable again. The values of $D_{\rm sim}$ shown in Fig. 5(a) were obtained from exponential fits to the time interval $100 \leq t \leq 200$. For much larger times the system reaches the correlated equilibrium state described by $f_i(\mathbf{r}) = f_{\rm eq}$ and $G_{ij}(\mathbf{r},\mathbf{r}') = \mathcal{G}^{\rm eq}_{ij}(\mathbf{r}-\mathbf{r}')$.

As β increases further beyond $\beta_c(\text{Boltzmann})$ the deviations of the simulation data from $D_E(\beta)$ become larger and larger. The reason for this is that, as the value of $D_E(\beta)$ gets closer to zero, the influence of third and higher order correlations (which are completely neglected in this article) becomes more and more important. A qualitative explanation is the following. At each time step all *pair* correlations are damped by a factor $\|\Gamma(\mathbf{q})\|^2 \simeq e^{-2Dq^2}$, while the *triplet* correlations are damped by a factor $\|\Gamma(\mathbf{q})\|^3 \simeq e^{-3Dq^2}$. As $D \to 0$ "critical slowing down" occurs due to the divergence of the

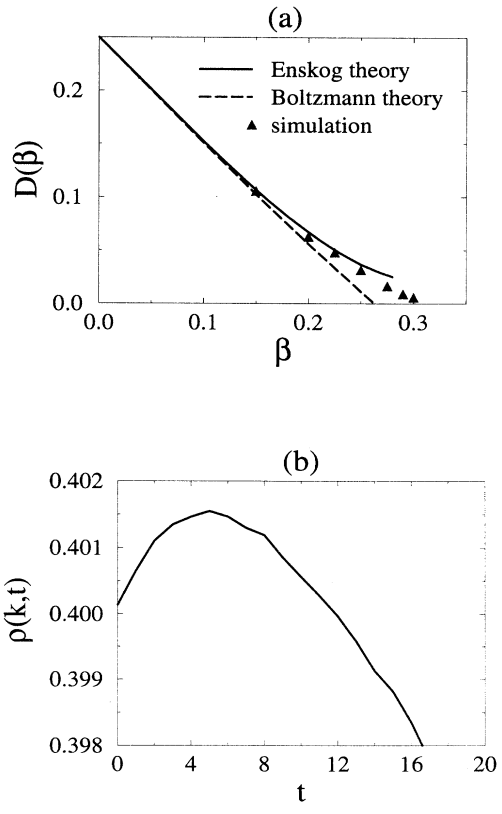

FIG. 5. (a) Comparison between the predictions for the diffusion coefficient $D(\beta)$ obtained from Boltzmann theory and self-consistent Enskog theory, and simulation results, for $f_{\rm eq} = \frac{1}{2}$. (b) Time evolution of Fourier component $\rho(\mathbf{k},t)$ for $\beta = 0.3$ satisfying $\beta_c(\text{Boltzmann}) < \beta < \beta_c$.

time scale of relaxation, $\tau = 1/(Dq^2) \to \infty$. As a consequence, pair and triple correlations become of equal importance. Numerically, this phenomenon manifests itself through the fact that the iterative scheme becomes unstable for $\beta > 0.28$. This makes it very difficult to extract a critical value β_c(Enskog).

VI. TIME EVOLUTION OF THE STRUCTURE FACTOR

When $\beta > \beta_c$ the spatially homogeneous state is not the equilibrium state. Instead, the system tries to reach a completely phase separated state where a high density phase is in coexistence with a low density phase. The system reaches this state through a process of coarsening, where it reaches local equilibrium on larger and larger length scales.

The static structure factor $S(\mathbf{q},t)$, defined as the Fourier transform of the density-density correlation function $\mathcal{G}_{\rho\rho}(\mathbf{q},t) = \sum_{ij} \mathcal{G}_{ij}(\mathbf{q},t)$, is a convenient quantity for characterizing the morphology of the density pattern in a statistical sense. It is given by

$$S(\mathbf{q},t) = \left\langle |\delta\rho(\mathbf{q},t)|^2 \right\rangle = \sum_{ij} \hat{\mathcal{G}}_{ij}(\mathbf{q},t). \tag{77}$$

By a slight modification of the theory in Sec. V A we can calculate the time evolution of $\hat{\mathcal{G}}_{ij}(\mathbf{q},t)$. In Sec. V A the equilibrium value of the excess pair correlation function $\hat{C}^{\rm eq}_{ij}(\mathbf{q})$ in the stable regime $\beta < \beta_c$ was obtained as a superposition of contributions from sources $\hat{B}(\mathbf{q},t_0)$ at all previous times t_0, as expressed by Eq. (55). An alternative way of stating the theory of Sec. V A is to say that the excess correlation function $\hat{C}_{ij}(\mathbf{q},t)$ evolves according to

$$\hat{C}_{ij}(\mathbf{q},t+1) = \sum_{k\ell} \Gamma^E_{ik}(\mathbf{q})\Gamma^E_{j\ell}(-\mathbf{q})\hat{C}_{k\ell}(\mathbf{q},t) + S_i(\mathbf{q})S_j(-\mathbf{q})\hat{B}_{ij}(\mathbf{q},t), \tag{78}$$

where the Enskog propagator $\Gamma^E_{ik}(\mathbf{q})$ depends on t through $C_{ij}(\mathbf{r},t)$, the inverse Fourier transform of $\hat{C}_{ij}(\mathbf{q},t)$.

Let us assume that at $t = 0$ the system is prepared in a completely random initial state so that $\hat{C}_{ij}(\mathbf{q},0) = 0$. We can then obtain $S(\mathbf{q},t)$ for all $t \geq 0$ by iterating Eq. (78) while evaluating $C_{ij}(\mathbf{r},t)$ at each time step to calculate $\Gamma^E_{ik}(\mathbf{q},t)$. This defines an Enskog-type prediction $S_E(\mathbf{q},t)$ for the evolution of $S(\mathbf{q},t)$.

An alternative and much simpler approach is the so-called Cahn-Hilliard theory [19] which states that all fluctuations $\delta s_i(\mathbf{q},t)$ evolve according to Boltzmann theory as

$$\delta s_i(\mathbf{q},t+1) = \sum_k \Gamma^B_{ik}(\mathbf{q})\delta s_k(\mathbf{q},t), \tag{79}$$

so that the structure factor is given by

$$\begin{aligned} S_{\rm CH}(\mathbf{q},t) &= \sum_{ij,k\ell} \left[\Gamma^B(\mathbf{q})\Gamma^B(-\mathbf{q})\right]^t_{ij,k\ell} \\ &\quad \times \langle \delta s_k(\mathbf{q},0)\delta s_\ell(-\mathbf{q},0)\rangle \\ &= b g_{\rm eq} \left| \sum_i \psi_D(\mathbf{q}) \right|^2 e^{2z_D(\mathbf{q})t}. \end{aligned} \tag{80}$$

Here we have used $\langle \delta s_k(\mathbf{q},0)\delta s_\ell(-\mathbf{q},0)\rangle = b g_{\rm eq}\delta_{k\ell}$ together with Eq. (30).

In Fig. 6 the Enskog theory is compared with simulations for an $L = 512$ system with $f_{\rm eq} = \frac{1}{2}$ and $\beta = \frac{1}{2} > \beta_c$. We have plotted the circular average $S(q,t)$ of the structure factor $S(\mathbf{q},t)$. This is useful even though $S(\mathbf{q},t)$ is strongly anisotropic, as was explained in Sec. III C. At $t = 1$ the Enskog prediction $S_E(\mathbf{q},1) = \sum_{ij} S_i(\mathbf{q})S_j(-\mathbf{q})\hat{B}_{ij}(\mathbf{q},0)$ is exact because the initial state is completely factorized. As can be seen from Fig. 6, Enskog theory gives an excellent prediction of $S(q,t)$ up to $t \simeq 15$. For larger times the theory breaks down.

From Fig. 7 it is clear that Cahn-Hilliard theory is incapable of predicting the dynamics of $S(q,t)$ even for small times. At $t = 5$ the predicted value $S_{\rm CH}(q,5)$ is

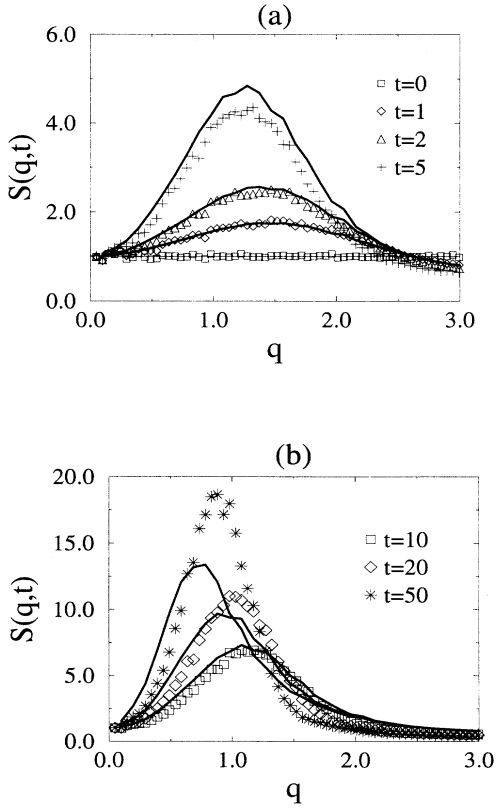

FIG. 6. Enskog theory for $S(q,t)$ (solid lines) compared with simulation results (symbols). The theory gives a good prediction of the time evolution up to $t \simeq 15$.

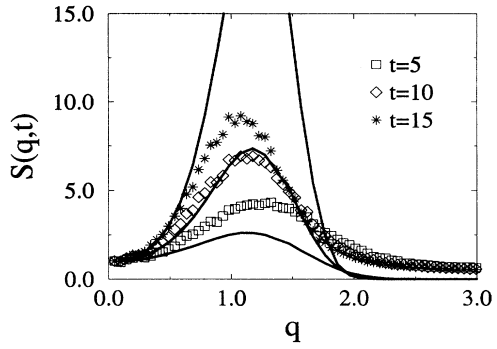

FIG. 7. Cahn-Hilliard theory for $S(q,t)$ (solid lines) compared with simulation results (symbols). The agreement at $t = 10$ is accidental.

too small by a factor of 2. However, $S_{\rm CH}(q,t)$ grows exponentially according to Eq. (80). At $t = 10$ there is a coincidental agreement but at $t = 15$ the Cahn-Hilliard prediction is already too large by a factor of 10.

A surprising feature of the Enskog theory is that it predicts some of the coarsening at short times, i.e., the shifting of the maximum of $S(q,t)$ to smaller q values as time increases. This is essentially a nonlinear effect. The reason for it to occur is that the Enskog propagator $\Gamma^E_{ik}(\mathbf{q},t)$ in Eq. (78) itself contains terms linear in $\hat{C}_{ij}(\mathbf{q},t)$. Consequently Eq. (78) contains quadratic and cubic terms that lead to a coupling between different Fourier components $\mathbf{q}$.

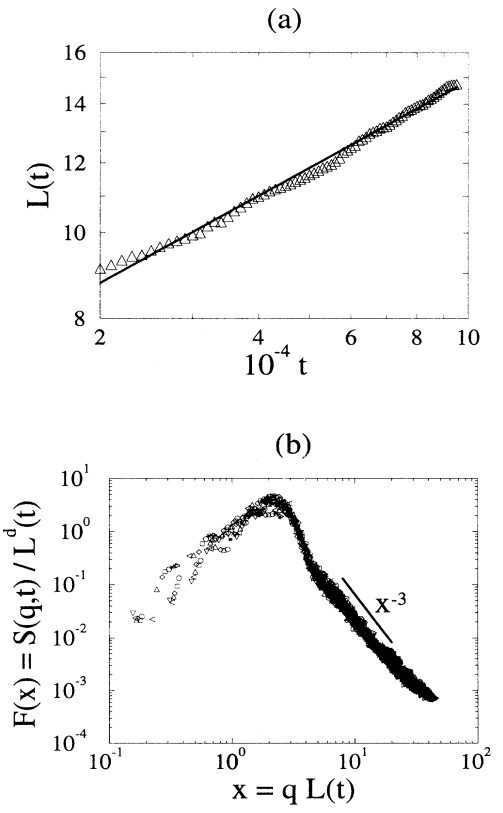

FIG. 8. (a) Power law growth of the characteristic length scale $L(t) \sim t^{1/3}$. (b) Scaling function $F(x)$ obtained as a collapse plot of scaled structure function $S(k,t)$ for times t from $t = 500$ up to $t = 10^5$. For large x Porod's law, $F(x) \sim x^{-3}$, is satisfied.

For large times the model exhibits *dynamical scaling*,

$$S(q,t) = [L(t)]^d F(qL(t)), \tag{81}$$

with $d = 2$ the dimensionality, $F(x)$ a scaling function, and $L(t)$ a typical length scale that is conveniently defined as the first zero of the circularly averaged density-density correlation function $\mathcal{G}_{\rho\rho}(r,t)$. Dynamical scaling is expected to hold when the pattern morphology is determined by a single length scale $L(t)$. This means that the typical width of the interfaces connecting regions of high and low density must be small compared to $L(t)$. In the scaling regime, power law growth is observed consistent with the Lifshitz-Slyosov-Wagner prediction $L(t) \sim t^{1/3}$ [19]. This behavior is typical for the late stages of phase separation in diffusive models with a scalar order parameter.

In Fig. 8(a) we have plotted $L(t)$ on a log-log scale. A power law fit to the time interval $2 \times 10^4 \leq t \leq 10^5$ yields $L(t) \sim t^z$, with $z = 0.33 \pm 0.03$. In Fig. 8(b) the scaling form Eq. (81) is tested by collapsing data for times from $t = 500$ up to $t = 10^5$. As a simple consequence [20] of the sharpness of the interfaces between domains on the scale of $L(t)$, the scaling function $F(x)$ should obey *Porod's law* for large x,

$$F(x) \sim x^{-(d+1)}. \tag{82}$$

A fit to the interval $7 \leq x \leq 17$ yields $F(x) \sim x^{-\alpha}$ with $\alpha = 2.9 \pm 0.2$. Similar measurements were already performed in Ref. [17], where the first moment of the structure factor was used to define a characteristic length scale. However, due to the more convincing collapse of data in Fig. 8(b), especially for large x, we have been able to verify Porod's law. The crossover from Porod's law to more complicated behavior occurs at a value of x that is approximately equal to three times the location of the maximum of $F(x)$. This is consistent with independent experimental results [21].

VII. DISCUSSION

In this article we have formulated a theory for spatial correlations in lattice-gas automata lacking detailed balance. We have successfully applied the theory to calculate corrections to mean-field theory for a pattern-forming diffusive model, in both the spatially stable and unstable parameter regimes.

We started by formulating a mean-field theory in Sec. III for the model with nearest neighbor interaction defined in Sec. II. The theory was applied to obtain an expression for the diffusion coefficient $D(\beta)$ in terms of a few matrix elements depending on the inverse temperature parameter β. An approximate analytical expression

for these matrix elements was obtained by performing a "high temperature expansion" around $\beta = 0$. The prediction for the critical inverse temperature $\beta_c \simeq 0.263$, defined by $D(\beta_c) \equiv 0$, that we obtained from mean-field theory for the half-filled lattice does not agree with the value $\beta_c = 0.30$–0.35 obtained from a block spin analysis by Alexander *et al.* [17], and in this article by observing the decay of a sinusoidal density perturbation.

The macroscopic behavior of the model can be understood in terms of a single diffusive mode, with an eigenvalue $z_D(\mathbf{k})$, which becomes unstable for $\beta > \beta_c$. By studying the decay rate $z_D(\mathbf{k})$ of the diffusive mode as a function of the wave vector $\mathbf{k}$ for both the square and the triangular lattices we could give a clear explanation of the observed anisotropy on the square lattice, and the near isotropy on the triangular lattice.

By considering the effect of an external driving field in the mean-field approximation we were able to explain the observation in Ref. [17] of a striped phase with structure perpendicular to the direction of the driving field, and the reported suppression of the critical temperature. A study of the diffusive eigenvalue $z_D(\mathbf{k})$ in the $\mathbf{k}$ plane provides a detailed scenario for the changing behavior of the model for different temperatures at fixed driving field. In addition we derived a linear response relation between the strength of the driving field and the induced particle flux, with a susceptibility that is proportional to the variance of the particle flux in the absence of the driving field, in good agreement with simulation results.

To explain the discrepancy between the mean-field prediction for β_c and the simulation value, we developed in Sec. V a theory for the static pair correlation function in equilibrium and its effect on the value of the diffusion coefficient. We found that for $\beta < \beta_c$ not too close to the critical point our theory explains an important part of the deviation from mean-field theory. Near the critical point $\beta = \beta_c$, however, our calculation of the pair correlation function breaks down. The typical relaxation time in the system, which is inversely proportional to the diffusion coefficient D, diverges at the critical point since $D \to 0$ for $\beta \to \beta_c$. As a consequence of this critical slowing down higher order correlations become dominant. Still, the theory provides a qualitative explanation of the deviation from the mean-field value of β_c.

The method discussed in Sec. V for calculating equilibrium pair correlations in the stable parameter range $\beta < \beta_c$ was adapted in Sec. VI for the case $\beta > \beta_c$, to predict for *short* times the time evolution of the static structure factor $S(q,t)$, starting from a completely random initial state. It was found that the Enskog theory can successfully predict $S(q,t)$ for times up to $t \simeq 15$. Even for this short time regime there is a dramatic improvement with respect to a Cahn-Hilliard-type theory which assumes that all modes evolve independently. Surprisingly, the Enskog theory accounts for some of the nonlinearity that leads to coarsening. This feature is completely absent in Cahn-Hilliard theory, where the fastest growth of $S(q,t)$ occurs at the same wave number q_m for all times.

Finally, we performed simulations on an $L = 256$ lattice to test the predictions of dynamical scaling and power law growth of the characteristic length scale $L(t)$ for *large* times. Such measurements were already performed in Ref. [17], but we have found a more convincing indication of scaling, over a much longer time range. In addition, we were able to verify Porod's law for the large wave number behavior of the scaling function, which is an important indication of the separation of length scales between the typical domain size and the average width of the interface between domains. It may well be possible that this improvement is due to the fact that we have used the first zero of the pair correlation function as a characteristic length scale, rather than the first moment of the structure function $S(q,t)$, as was done in Ref. [17].

Although all calculations in this article were specialized to the particular model we have chosen to analyze here, the method is quite general and can be applied to a large class of lattice-gas automata with short range interactions between nodes, including models with strictly local collision rules. In particular, we expect that the theory can be successfully applied to reaction-diffusion models to explain deviations from the (mean-field) rate equations in the diffusion-limited regime, where correlated fluctuations play an important role. Another possible application is to models for traffic jams where in some cases mean-field theory fails to predict the parameter dependence observed in simulations [5,6].

ACKNOWLEDGMENTS

It is a pleasure to thank Professor M. H. Ernst for his advice and encouragement, as well as for a critical reading of the manuscript. This work was financially supported by the "Stichting voor Fundamenteel Onderzoek der Materie" (FOM), which is sponsored by the "Nederlandse Organisatie voor Wetenschappelijk Onderzoek" (NWO).

APPENDIX A: LINEARIZED BOLTZMANN OPERATOR

In this Appendix we discuss the structure of the collision matrices given by [see Eq. (21)],

$$\Omega_{ik}^{11,p} = \left\langle [\delta\sigma_i(\mathbf{r}) - \delta s_i(\mathbf{r})] \frac{\delta s_k(\mathbf{r}+\mathbf{c}_p)}{f^{\mathrm{eq}}(1-f^{\mathrm{eq}})} \right\rangle_{\mathrm{MF,eq}}$$

$$= \sum_{\sigma(\mathbf{r})} \sum_{\{s(\mathbf{r}+\mathbf{c}_p)\}} [\delta\sigma_i(\mathbf{r}) - \delta s_i(\mathbf{r})] \frac{\delta s_k(\mathbf{r}+\mathbf{c}_p)}{f^{\mathrm{eq}}(1-f^{\mathrm{eq}})}$$

$$\times A_{s(\mathbf{r}),\sigma(\mathbf{r})}(\mathbf{G}(\mathbf{r})) \prod_{p=0}^{b} F(s(\mathbf{r}+\mathbf{c}_p)), \qquad \text{(A1)}$$

that occur in the linearized Boltzmann equation Eq. (20).

We start by summarizing the results. For $p = 0$ we find that $\Omega^{11,0}$ is independent of both β and $f^{\rm eq}$,

$$\Omega^{11,0}_{ik} = \frac{1}{b} - \delta_{ik}. \tag{A2}$$

For $1 \le p \le b$ it is sufficient to give the structure of $\Omega^{11,1}$ only since all other matrices $\Omega^{11,p}$ are related to the first by rotational symmetry. On the square lattice the general structure of $\Omega^{11,1}$ is given by

$$\Omega^{11,1} = \begin{pmatrix} A-B & A-B & A-B & A-B \\ B & B & B & B \\ -A-B & -A-B & -A-B & -A-B \\ B & B & B & B \end{pmatrix}, \tag{A3}$$

with $B = 0$ on the half-filled lattice ($f = \frac{1}{2}$). On the triangular lattice the general structure of $\Omega^{11,1}$ is given by

$$\Omega^{11,1} = \begin{pmatrix} A-2C & A-2C & A-2C & A-2C & A-2C & A-2C \\ B+C & B+C & B+C & B+C & B+C & B+C \\ -B+C & -B+C & -B+C & -B+C & -B+C & -B+C \\ -A-2C & -A-2C & -A-2C & -A-2C & -A-2C & -A-2C \\ -B+C & -B+C & -B+C & -B+C & -B+C & -B+C \\ B+C & B+C & B+C & B+C & B+C & B+C \end{pmatrix}, \tag{A4}$$

with $C = 0$ on the half-filled lattice. Of course all matrix elements in Eqs. (A3) and (A4) vanish when $\beta = 0$.

In the remainder of this Appendix we prove these results. To prove Eq. (A2) we split

$$\langle [\delta\sigma_i(\mathbf{r}) - \delta s_i(\mathbf{r})]\delta s_k(\mathbf{r})\rangle = \langle \delta\sigma_i(\mathbf{r})\delta s_k(\mathbf{r})\rangle - \langle \delta s_i(\mathbf{r})\delta s_k(\mathbf{r})\rangle. \tag{A5}$$

For the second term we have $\langle \delta s_i(\mathbf{r})\delta s_k(\mathbf{r})\rangle = g_{\rm eq}\delta_{ik}$. To evaluate the first term we note that the outcome of a collision only depends on $s(\mathbf{r})$ through $\rho(\mathbf{r})$, so that $\langle \delta\sigma_i(\mathbf{r})\delta s_k(\mathbf{r})\rangle$ does not depend on i or k and

$$\langle \delta\sigma_i(\mathbf{r})\delta s_k(\mathbf{r})\rangle = \frac{1}{b^2}\langle [\delta\rho(\mathbf{r})]^2\rangle = \frac{1}{b} g_{\rm eq}, \tag{A6}$$

where we have used $\rho(s) = \rho(\sigma)$. Combining these results we obtain Eq. (A2).

Next we turn to the symmetry properties of $\Omega^{11,1}$ in Eqs. (A3) and (A4). Again these matrices do not depend on the second index j because the outcome of a collision only depends on the states $s(\mathbf{r} + \mathbf{c}_p)$ of the neighboring nodes through the density $\rho(\mathbf{r} + \mathbf{c}_p)$. The matrices $\Omega^{11,p}$ have all symmetries of the underlying lattice. Let π denote a permutation of the set $\{\mathbf{c}_i\}$ of nearest neighbor vectors, corresponding to a particular rotation or reflection symmetry of the lattice. We then have

$$\Omega^{\pi(m)}_{\pi(i),\pi(j)} = \Omega^m_{ij}. \tag{A7}$$

In particular we have the rotational symmetries

$$\Omega^{11,p+1}_{i+1,k+1} = \Omega^{11,p}_{ik} \tag{A8}$$

that relate $\Omega^{11,1}$ to the other $\Omega^{11,p}$ with $2 \le p \le b$. To obtain the internal symmetries of $\Omega^{11,1}$ we consider reflection in the x axis where $\pi(\mathbf{c}_1) = \mathbf{c}_1$. On the square lattice we have $\Omega^{11,1}_{2,k} = \Omega^{11,1}_{4,k}$ yielding Eq. (A3). On the triangular lattice both $\Omega^{11,1}_{2,k} = \Omega^{11,1}_{6,k}$ and $\Omega^{11,1}_{3,k} = \Omega^{11,1}_{5,k}$ hold, which leads to Eq. (A4).

In the special case of the half-filled lattice, the distribution function $F(s)$ reduces to a trivial factor 2^{-b}. As a consequence the matrices $\Omega^{11,p}_{ik}$ will possess an additional symmetry, $\Omega^{11,p}_{i+b/2,j} = -\Omega^{11,p}_{i,j}$. The proof of this goes as follows. First we note that $\Omega^m_{i+b/2,j} = \Omega^{m-b/2}_{i,j}$. We proceed by making the substitutions $s_i(\mathbf{r}) \Rightarrow 1 - s_i(\mathbf{r})$, $\sigma_i(\mathbf{r}) \Rightarrow 1 - \sigma_i(\mathbf{r})$, and $s_j(\mathbf{r} + \mathbf{c}_m) \Rightarrow s_j(\mathbf{r} - \mathbf{c}_m)$, so that $\mathbf{J}(\sigma) \Rightarrow -\mathbf{J}(\sigma)$ and $\mathbf{G}(\mathbf{r}) \Rightarrow -\mathbf{G}(\mathbf{r})$, and observe that $A_{s\sigma}(\mathbf{G}(\mathbf{r}))$ is invariant under these substitutions. We can then derive

$$\begin{aligned} \Omega^{11,p+b/2}_{ik} &= \left\langle [\delta\sigma_i(\mathbf{r}) - \delta s_i(\mathbf{r})] \frac{\delta s_k(\mathbf{r} - \mathbf{c}_p)}{g_{\rm eq}} \right\rangle \\ &\Rightarrow -\left\langle [\delta\sigma_i(\mathbf{r}) - \delta s_i(\mathbf{r})] \frac{\delta s_k(\mathbf{r} + \mathbf{c}_p)}{g_{\rm eq}} \right\rangle \\ &= -\Omega^{11,p}_{ik}. \end{aligned} \tag{A9}$$

It follows that on the half-filled square ($b = 4$) lattice $\Omega^{11,1}_{21} = 0$, so that $B = 0$ in Eq. (A3). On the half-filled triangular ($b = 6$) lattice we have $\Omega^{11,1}_{21} + \Omega^{11,1}_{51} = 0$, so that $C = 0$ in Eq. (A4).

APPENDIX B: HIGH TEMPERATURE EXPANSION

In this Appendix we show how to expand $\Omega^{11,1}_{11}(\beta)$ up to linear order in β. This approximation gives quite reasonable results, as is shown in the body of this article. We only perform the expansion for the special case of the half-filled square lattice where $f = \frac{1}{2}$ and $b = 4$. The result of our calculation will be that $\Omega^{11,1}_{11}(\beta) = \frac{1}{4}\beta + O(\beta^2)$.

In lowest order we may approximate $e^{\beta \mathbf{J}(\sigma)\cdot\mathbf{G}} \simeq 1 + \beta \mathbf{J}(\sigma)\cdot\mathbf{G}$, so that expression Eq. (6) for the transition matrix $A_{s\sigma}(\mathbf{G})$ takes the form

$$A_{s\sigma}(\mathbf{G}) \simeq \frac{[1+\beta \mathbf{J}(\sigma)\cdot\mathbf{G}]\delta(\rho(\sigma),\rho(s))}{\sum_\sigma \delta(\rho(\sigma),\rho(s))}. \tag{B1}$$

Note that the normalization factor occurring in this expression can be written as

$$\sum_\sigma \delta(\rho(\sigma)-\rho(s)) = \binom{4}{\rho(s)} \equiv \frac{4!}{\rho(s)![4-\rho(s)]!}. \tag{B2}$$

For later reference we recall that

$$\sum_{\rho=0}^{4} \binom{4}{\rho} = 2^4, \qquad \sum_{\rho=0}^{4} \rho \binom{4}{\rho} = 2^5,$$
$$\sum_{\rho=0}^{4} \rho^2 \binom{4}{\rho} = 5\times 2^4. \tag{B3}$$

Let s and σ denote the pre- and postcollision states at node $\mathbf{r}$, and let s^p and ρ^p denote the precollision state and density at the nearest neighbors $\mathbf{r}+\mathbf{c}_p$. For $f=\frac{1}{2}$ the factorized node distribution function $F(s)$ reduces to a factor 2^{-4} independent of s. Starting from the definition of $\Omega_{11}^{11,1}$ in Eq. (21) we use the fact that $\Omega_{ik}^{11,p}$ does not depend on its second index k to obtain

$$\begin{aligned}\Omega_{11}^{11,1} &= \left\langle (\sigma_1 - s_1)\frac{\rho^1-2}{4g_{\mathrm{eq}}}\right\rangle_{\mathrm{MF,eq}} \\ &= \sum_{s\sigma}\sum_{s^1,\ldots,s^4} (\sigma_1-s_1)(\rho^1-2)A_{s\sigma}(\mathbf{G})F(s)F(s^1)\cdots F(s^4) \\ &= \sum_{s\sigma}\sum_{\rho^1,\ldots,\rho^4} (\sigma_1-s_1)(\rho^1-2)[1+\beta\mathbf{J}(\sigma)\cdot\mathbf{G}]\binom{4}{\rho(s)}^{-1}\delta(\rho(\sigma),\rho(s))\frac{1}{2^{20}}\binom{4}{\rho^1}\cdots\binom{4}{\rho^4}.\end{aligned} \tag{B4}$$

Using $\mathbf{J}(\sigma)\cdot\mathbf{G} = (\sigma_1-\sigma_3)(\rho^1-\rho^3)+(\sigma_2-\sigma_4)(\rho^2-\rho^4)$ and leaving out terms that vanish due to symmetries we obtain

$$\begin{aligned}\frac{\Omega_{11}^{11,1}}{\beta} &= \frac{1}{2^{20}}\left[\sum_{\rho^1\rho^3}\binom{4}{\rho^1}\binom{4}{\rho^3}\rho^1(\rho^1-\rho^3)\right]\left[\sum_{s\sigma}(\sigma_1-s_1)(\sigma_1-\sigma_3)\binom{4}{\rho(s)}^{-1}\delta(\rho(\sigma),\rho(s))\right] \\ &= \frac{1}{2^4}\left[\sum_{s\sigma}(\sigma_1-s_1)(\sigma_1-\sigma_3)\binom{4}{\rho(s)}^{-1}\delta(\rho(\sigma),\rho(s))\right].\end{aligned} \tag{B5}$$

For the last equality we have made use of Eq. (B3). Working out in detail the remaining expression between parentheses we obtain the final result $\Omega_{11}^{11,1} = \frac{1}{4}\beta$.

APPENDIX C: LINEAR RESPONSE THEOREM

In this Appendix we derive an expression for the susceptibility χ describing the linear response $\langle \mathbf{J}(\sigma)\rangle_{\mathbf{E}}$ of the system to a small external driving field $\mathbf{E}$. The general linear response relation reads

$$\langle J_\alpha(\sigma)\rangle_{\mathbf{E}} = \chi_{\alpha\beta}E_\beta = \chi E_\alpha, \tag{C1}$$

where the second rank tensor $\chi_{\alpha\beta} = \chi\delta_{\alpha\beta}$ is isotropic, both on the square and on the triangular lattice. The calculation in this appendix is performed within the mean-field approximation; no static correlations are taken into account.

The field $\mathbf{E}$ induces a spatially homogeneous deviation from the field-free equilibrium state $f_i(\mathbf{r}|\mathbf{E}=\mathbf{0}) = f_{\mathrm{eq}}$ of the form

$$f_i(\mathbf{r}|\mathbf{E}) = f_{\mathrm{eq}} + \delta f_i(\mathbf{E}), \tag{C2}$$

giving rise to an average flux

$$\langle \mathbf{J}(\sigma)\rangle_{\mathbf{E}} = \sum_{i=1}^{b} \mathbf{c}_i \delta f_i(\mathbf{E}). \tag{C3}$$

For small $\mathbf{E}$ we expand Eqs. (37) and (38) as

$$A_{s\sigma}(\mathbf{G},\mathbf{E}) \simeq A_{s\sigma}(\mathbf{G})\left\{1+[\mathbf{J}(\sigma)-\overline{\mathbf{J}(\sigma)}]\cdot\mathbf{E}\right\}, \tag{C4}$$

where we have defined the expectation value of $\mathbf{J}(\sigma)$ averaged over all possible outcomes σ of a collision taking place at given fixed s and $\mathbf{G}$ as

$$\overline{\mathbf{J}(\sigma)} \equiv \sum_\sigma \mathbf{J}(\sigma)A_{s\sigma}(\mathbf{G}). \tag{C5}$$

In the mean-field approximation the deviations $\delta f_i(\mathbf{E})$ are implicitly defined as the stationary solution to the nonlinear Boltzmann equation for given $\mathbf{E}$, i.e.,

$$\Omega_i^{10}[f_{\mathrm{eq}} + \delta f(\mathbf{E})] \equiv 0. \tag{C6}$$

Using Eqs. (12), (17), and (C4) we expand Eq. (C6)

around $\mathbf{E}=\mathbf{0}$ obtaining

$$\sum_j \frac{\partial \Omega_i^{10}}{\partial f_j}\delta f_j(\mathbf{E}) + \left\langle (\sigma_i - s_i)[\mathbf{J}(\sigma) - \overline{\mathbf{J}(\sigma)}]\right\rangle_{\mathrm{MF,eq}} \cdot \mathbf{E} = 0. \tag{C7}$$

Now observe that

$$\frac{\partial \Omega_i^{10}}{\partial f_j} = \sum_{p=0}^{b} \left.\frac{\partial \Omega_i^{10}(\mathbf{r})}{\partial f_j(\mathbf{r}+\mathbf{c}_p)}\right|_{\mathrm{eq}} = \Omega_{ij}^{11,0} + \sum_{p=1}^{b} \Omega_{ij}^{11,p} = \Omega_{ij}^{11,0}, \tag{C8}$$

so that we arrive at the following linear equation from which $\delta f_i(\mathbf{E})$ must be solved for given $\mathbf{E}$:

$$\sum_j \Omega_{ij}^{11,0}\delta f_j(\mathbf{E}) + \left\langle (\sigma_i - s_i)[\mathbf{J}(\sigma) - \overline{\mathbf{J}(\sigma)}]\right\rangle_{\mathrm{MF,eq}} \cdot \mathbf{E} = 0. \tag{C9}$$

Solving this equation involves inversion of the symmetric matrix $\Omega_{ij}^{11,0} = 1/b - \delta_{ij}$ (see Appendix A). This matrix has null space spanned by the vector $(1,1,\ldots,1)$ which corresponds to the required conservation of particle number during collision expressed by

$$\sum_i \delta f_i(\mathbf{E}) = 0. \tag{C10}$$

We must solve Eq. (C9) while satisfying the constraint Eq. (C10), which enables us to invert $\Omega^{11,0}$ within the orthogonal complement of the null space. In particular, it can be verified that since $c_{\alpha i}$ with $\alpha = x, y$ is an eigenvector of $\Omega^{11,0}$ with eigenvalue -1 we have

$$\sum_j \left[\frac{1}{\Omega^{11,0}}\right]_{ij} c_{\alpha j} = -c_{\alpha i}. \tag{C11}$$

Combining Eqs. (C3) and (C9) we obtain

$$\begin{aligned}\langle J_\alpha(\sigma)\rangle_{\mathbf{E}} &= -\sum_{i,j=1}^{b} c_{\alpha i}\left[\frac{1}{\Omega^{11,0}}\right]_{ij} \\ &\quad\times \left\langle (\sigma_j - s_j)[J_\beta(\sigma) - \overline{J_\beta(\sigma)}]\right\rangle_{\mathrm{MF,eq}} E_\beta \\ &= \sum_{i=1}^{b} c_{\alpha i}\left\langle (\sigma_i - s_i)[J_\beta(\sigma) - \overline{J_\beta(\sigma)}]\right\rangle_{\mathrm{MF,eq}} E_\beta,\end{aligned} \tag{C12}$$

where Eq. (C11) has been used once more. We consider two parts of this expression separately. On the one hand, introducing

$$\overline{\mathbf{J}^2(\sigma)} \equiv \sum_\sigma [\mathbf{J}(\sigma)]^2 A_{s\sigma}(\mathbf{G}), \tag{C13}$$

we have

$$\begin{aligned}&\sum_i c_{\alpha i}\langle (\sigma_i - s_i) J_\beta(\sigma)\rangle_{\mathrm{MF,eq}} \\ &\quad= \sum_{ij} c_{\alpha i}c_{\beta j}\langle (\delta\sigma_i - \delta s_i)\delta\sigma_j\rangle_{\mathrm{MF,eq}} \\ &\quad= \sum_{ij} c_{\alpha i}c_{\beta j}\langle \delta\sigma_i\delta\sigma_j\rangle_{\mathrm{MF,eq}} \\ &\quad= \tfrac{1}{2}\delta_{\alpha\beta}\left\langle \overline{\mathbf{J}^2(\sigma)}\right\rangle_{\mathrm{MF,eq}}.\end{aligned} \tag{C14}$$

On the other hand,

$$\begin{aligned}&\sum_i c_{\alpha i}\left\langle (\sigma_i - s_i)\overline{J_\beta(\sigma)}\right\rangle_{\mathrm{MF,eq}} \\ &\quad= \tfrac{1}{2}\delta_{\alpha\beta}\sum_\gamma\sum_i c_{\gamma i}\left\langle (\sigma_i - s_i)\overline{J_\gamma(\sigma)}\right\rangle_{\mathrm{MF,eq}} \\ &\quad= \tfrac{1}{2}\delta_{\alpha\beta}\left\langle [\mathbf{J}(\sigma) - \mathbf{J}(s)]\cdot\overline{\mathbf{J}(\sigma)}\right\rangle_{\mathrm{MF,eq}} \\ &\quad= \tfrac{1}{2}\delta_{\alpha\beta}\left\langle \overline{\mathbf{J}(\sigma)}^2\right\rangle_{\mathrm{MF,eq}}.\end{aligned} \tag{C15}$$

In deriving Eqs. (C14) and (C15) we have used the fact that, if the collision rules of a LGA satisfy all symmetries of the square or the triangular lattice in $d=2$ dimensions, tensors of rank 2, $T_{\alpha\beta}$, are isotropic, i.e., $T_{\alpha\beta} = T\delta_{\alpha\beta}$ with $T = \frac{1}{d}\mathrm{Tr}(T_{\alpha\beta}) = \frac{1}{d}\sum_\gamma T_{\gamma\gamma}$.

Identification of Eq. (C12) with Eq. (C1) yields the following expression for the susceptibility:

$$\begin{aligned}\chi &= \tfrac{1}{2}\left\langle \overline{\mathbf{J}^2(\sigma)} - \overline{\mathbf{J}(\sigma)}^2\right\rangle_{\mathrm{MF,eq}} \\ &= \tfrac{1}{2}\sum_s\sum_{\mathbf{G}}\left(\overline{\mathbf{J}^2(\sigma)} - \overline{\mathbf{J}(\sigma)}^2\right)F(s)F(\mathbf{G}),\end{aligned} \tag{C16}$$

with

$$\begin{aligned}F(\mathbf{G}) = &\sum_{\{s(\mathbf{r}+\mathbf{c}_p)\}} \delta\left[\mathbf{G} - \sum_{p=1}^{b}\mathbf{c}_p\rho(\mathbf{r}+\mathbf{c}_p)\right] \\ &\times\prod_{p=1}^{b} F(s)(\mathbf{r}+\mathbf{c}_p).\end{aligned} \tag{C17}$$

Equation (C16) can be interpreted as a *linear response theorem* relating the susceptibility χ to the variance of the postcollision flux $\mathbf{J}(\sigma)$ for $\mathbf{E}=\mathbf{0}$. In the special case $\beta = 0$ the collision matrix $A_{s\sigma}(\mathbf{G})$ is independent of $\mathbf{G}$ so that

$$\begin{aligned}\chi = \chi_0 &= \tfrac{1}{2}\sum_s \overline{\mathbf{J}^2(\sigma)}F(s) \\ &= \tfrac{1}{2}\sum_{ij}\mathbf{c}_i\cdot\mathbf{c}_j\left(\sum_{s\sigma}\delta\sigma_i\delta\sigma_j A_{s\sigma}(\mathbf{0})F(s)\right) \\ &= \tfrac{1}{2}bg_{\mathrm{eq}}.\end{aligned} \tag{C18}$$

[1] D. Rothman and J. M. Keller, J. Stat. Phys. **52**, 1119 (1988).
[2] C. Appert and S. Zaleski, Phys. Rev. Lett. **64**, 1 (1990).
[3] R. Kapral, A. Lawniczak, and P. Masiar, J. Chem. Phys. **96**, 2762 (1992).
[4] X.-G. Wu and R. Kapral, Phys. Rev. Lett. **70**, 1940 (1993).
[5] O. Biham, A. Middleton, and D. Levine, Phys. Rev. A **46**, 6124 (1992).
[6] J. M. Molera, F. C. Martinez, J. A. Cuesta, and R. Brito, Phys. Rev. E **51**, 175 (1995).
[7] A. K. Gunstensen, D. H. Rothman, S. Zaleski, and G. Zanetti, Phys. Rev. A **43**, 4320 (1991).
[8] A. K. Gunstensen and D. H. Rothman, Europhys. Lett. **18**, 157 (1992).
[9] R. Holme and D. H. Rothman, J. Stat. Phys. **68**, 409 (1992).
[10] H. J. Bussemaker, M. H. Ernst, and J. W. Dufty, J. Stat. Phys. **78**, 1521 (1995).
[11] R. Brito and M. H. Ernst, Phys. Rev. A **46**, 875 (1992).
[12] D. Frenkel and M. H. Ernst, Phys. Rev. Lett. **63**, 2165 (1989).
[13] M. Gerits, M. H. Ernst, and D. Frenkel, Phys. Rev. E **48**, 988 (1993).
[14] T. R. Kirkpatrick and M. H. Ernst, Phys. Rev. A **44**, 8051 (1991).
[15] T. Naitoh, M. H. Ernst, and J. W. Dufty, Phys. Rev. A **42**, 7187 (1990).
[16] G. A. van Velzen, R. Brito, and M. H. Ernst, J. Stat. Phys. **70**, 811 (1993).
[17] F. J. Alexander, I. Edrei, P. L. Garrido, and J. L. Lebowitz, J. Stat. Phys. **68**, 497 (1992).
[18] S. Chapman and T. G. Cowling, *The Mathematical Theory of Nonuniform Gases* (Cambridge University Press, Cambridge, England, 1970).
[19] J. S. Langer, in *Solids Far From Equilibrium*, edited by C. Godrèche (Cambridge University Press, Cambridge, England, 1992), p. 297.
[20] A. J. Bray, Physica A **194**, 41 (1993).
[21] K. Kubota, N. Kuwahara, H. Eda, and M. Sakazume, Phys. Rev. A **45**, 3377 (1992).

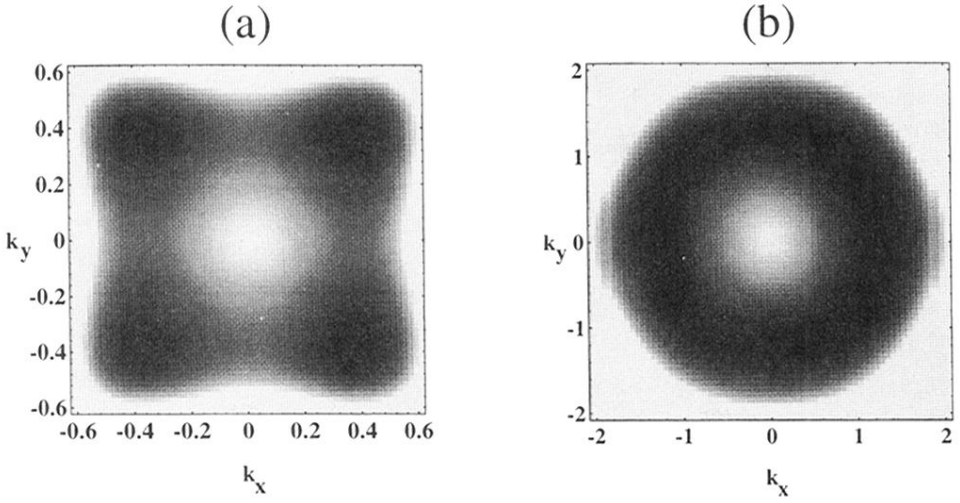

FIG. 2. Diffusive eigenvalue $z_D(\mathbf{k})$. Regions where $z_D(\mathbf{k}) > 0$ are indicated by gray scales: black denotes the fastest growing modes. (a) On the square lattice there exist strong anisotropies. (b) On the triangular lattice the spectrum is nearly isotropic.